

The following document is a pre-print version of:

Ross, P.-S., Goutier, J., Mercier-Langevin, P., et Dubé, B. (2011) Basaltic to andesitic volcanoclastic rocks in the Blake River Group, Abitibi Greenstone Belt: 1. Mode of emplacement in three areas. *Journal Canadien des Sciences de la Terre*, v. 48, p. 728-756

# Basaltic to andesitic volcanoclastic rocks in the Blake River Group, Abitibi Greenstone Belt: 1. Mode of emplacement in three areas

Pierre-Simon Ross  
INRS-ETE, 490 rue de la Couronne, Québec (QC), G1K 9A9, Canada

Jean Goutier  
Ministère des Ressources naturelles et de la Faune (Québec), 70 avenue Québec, Rouyn-Noranda (QC), J9X 6R1, Canada

Patrick Mercier-Langevin  
Geological Survey of Canada, 490 rue de la Couronne, Québec (QC), G1K 9A9, Canada

Benoît Dubé  
Geological Survey of Canada, 490 rue de la Couronne, Québec (QC), G1K 9A9, Canada

\* Corresponding author, [rossps@ete.inrs.ca](mailto:rossps@ete.inrs.ca)

## Abstract:

The Archean Blake River Group (BRG) of Ontario and Québec is dominated by submarine mafic to intermediate lavas, with more restricted felsic volcanic rocks. Given the good quality of outcrop, and high level of preservation of some BRG rocks, the mafic to intermediate lavas were used in the 1970s and 1980s to better understand the evolution of massive and pillowed submarine flows, and their associated fragmental facies (pillow breccias, hyaloclastite). Potentially, the BRG could also represent a useful volcanic succession for the study of explosive submarine eruption products in the ancient record. Before this is possible, however, a regional inventory of the mafic to intermediate volcanoclastic units is needed in order to clarify their characteristics and origins.

In this paper, we compare and contrast volcanoclastic rocks from three areas within the same formation of the northern BRG in Québec: the Monsabrais area, the *lac Duparquet* area, and the D'Alembert tuff area. Close examination reveals pronounced differences in terms of lateral continuity, thickness, grading, bedding, clast shapes, textures, etc. in the volcanoclastic rocks. These differences are interpreted to reflect vastly different emplacement

processes ranging from hyaloclastite generation as a result of self-fragmentation and lava contact with water (dominant in the Monsabrais and *lac Duparquet* areas) to aqueous density currents likely fed directly by explosive submarine eruptions (dominant in the D'Alembert tuff).

## Introduction

Explosive submarine volcanism – the importance of which has long been underestimated – is becoming an important topic in volcanology. White et al. (2003) provide an overview of the subject matter and Chadwick et al. (2008) describe a recent submarine explosive eruption filmed by a remotely operated vehicle. Furthermore, it is possible that some volcanogenic massive sulphide (VMS) deposits may be related to explosive submarine volcanism (e.g., Hudak et al. 2003; Franklin et al. 2005; Montelius et al. 2007).

The detailed study of subaqueous volcanoclastic deposits now exposed on land – for example, in the locally well exposed and well preserved Archean Blake River Group (BRG) of the Abitibi Greenstone Belt in Ontario and Québec – may contribute to a better understanding of submarine explosive eruptions, just as earlier detailed documentation of submarine

lava flows and their associated fragmental rocks in the BRG contributed to our comprehension of non-explosive subaqueous volcanism (e.g., Dimroth et al. 1978; Cousineau and Dimroth 1982).

As noted by White et al. (2003), however, understanding subaqueous eruptions from their deposits is challenging, and especially so for fragmental rocks. Interpreting the origin of volcanoclastic rocks spread over tens of kilometres from outcrops a few metres across is especially problematic, particularly when loose or variable terminology is employed, and numerous geologists are involved in the mapping over many years. Compilation of such observations can lead to inferred correlations (Mueller 2006; Pearson and Daigneault 2009) between rocks that in fact have nothing more in common than their fragmental character and a general mafic to intermediate geochemical composition. These correlations, and the megacaldera model that they led to in the BRG, would be incorrect if, for example, the volcanoclastic units occupied different stratigraphic positions, had different ages and geochemical compositions, and were produced by widely different processes ranging from explosive eruptions to hyaloclastite formation.

In order to use volcanoclastic rocks of the BRG to further improve our understanding of submarine explosive eruptive processes, we undertook a systematic field-based study of the main mafic to intermediate volcanoclastic units in the BRG using a consistent, modern terminology over the period 2006-2009. Our goals were to determine the physical characteristics, geochemical signatures, stratigraphic positions, ages, and origins of these rocks. A further aim of this investigation was to test whether the major volcanoclastic units were indeed correlative. In this paper, we describe in detail and interpret the mode of emplacement of some volcanoclastic rocks from the Renault-Dufresnoy Formation in the northern part of the BRG in Québec. Specifically, our work focussed on the D'Alembert tuff, the Monsabrais area, and the *lac* Duparquet area (Fig. 1). In a companion paper (Ross et al. 2010) we summarize the physical characteristics, inferred origins, age constraints and geochemical signatures of all the studied volcanoclastic units.

## **Geological setting and nomenclature**

### **The Blake River Group**

The BRG is the youngest (~2704-2695 Ma) dominantly volcanic package in the Abitibi Subprovince (Mortensen 1993; Corfu et al. 1989; Corfu 1993; Ayer et al. 2002; Lafrance et al. 2005; David et al. 2006; Thurston et al. 2008; FOOTNOTE 1). It consists largely of submarine, basaltic to rhyolitic, tholeiitic to calc-alkaline volcanic rocks,

including volcanoclastic rocks (Spence and de Rosen-Spence 1975; Goodwin 1977, 1982; Dimroth et al. 1982; Gélinas et al. 1984; Jensen and Langford 1985; Lafèche et al. 1992; Péloquin et al. 2008; Ross et al., 2008a), which are intruded by several generations of plutons and mafic to intermediate dykes and sills (Paradis et al. 1988; Galley and van Breemen 2002; Galley 2003; Piercey et al. 2008) (Fig. 1).

Based on about 40 U-Pb ages, Goutier et al. (2009) and FOOTNOTE 1, show that BRG rocks can be divided into the lower BRG (~2704-2699 Ma) and the upper BRG (~2699-2695 Ma). The BRG contains a significant number of VMS deposits, notably in the Noranda camp (e.g., Gibson and Watkinson 1990; Gibson and Galley 2007) including the large Horne and Quemont VMS deposits (e.g., Kerr and Gibson 1993) and LaRonde Penna in the Doyon-Bousquet-LaRonde camp (e.g., Dubé et al. 2007; Mercier-Langevin et al. 2007a, 2007b). Recent geochronological studies show that the Horne and Quemont VMS deposits belong to the lower BRG, whereas the VMS deposits in the Doyon-Bousquet-LaRonde camp and most of the Noranda camp belong to the upper BRG (Goutier et al. 2009; FOOTNOTE 1). This implies that VMS deposits were formed in several stages during the evolution of the BRG.

In many areas, metamorphic grade is low (greenschist and sub-greenschist facies; e.g., Powell et al. 1995), strong tectonic fabrics are absent, and hydrothermal alteration has not destroyed primary textures (e.g., Dimroth 1977; Hannington et al. 2003). This has made the BRG a favoured area for studies of submarine volcanism in ancient successions. Yet in some areas, alteration and/or deformation are intense enough to mask primary textures, and the overall geometry of the BRG is far from simple, including many folds and several generations of faults (Péloquin et al. 1990), some of which are thrust faults (e.g., Couture and Goutier 1996; Goutier 1997). In the volcanoclastic deposits we have studied, the dips of the strata vary from 10 to 90 degrees from horizontal, and the intensity of penetrative deformation varies from none to relatively intense.

### **Volcanoclastic units studied during the inventory**

The major mafic to intermediate volcanoclastic units we have examined in most detail are the D'Alembert tuff, the Stadacona member, and the Bousquet scoriaceous tuff (Ross et al. 2007, 2008b; Mercier-Langevin et al. 2008; Ross 2010; this paper) (Fig. 1c). Volcanoclastic rocks were also examined in detail around *lac* Monsabrais (Goutier et al. 2007a; Ross et al. 2008a; this paper), as well as around *lac* Labyrinthe and in Tannahill Township (Ross et al. 2009); in all of these cases, no major volcanoclastic units comparable to the D'Alembert tuff or the

Stadacona member were present. Mapping was performed around *lac* Duparquet (this paper) and finally, the Jévis Sud unit was briefly visited (Ross et al. 2007).

### Depositional setting of all volcanoclastic units

The only way to establish the depositional setting of all the volcanoclastic units in the BRG is to use bounding facies, since in some cases, the volcanoclastic rocks themselves do not display diagnostic criteria. All lava flows in the BRG are thought to have been emplaced in a submarine environment, given the abundance of pillow lavas and pillow breccias, the presence of many VMS deposits of different ages, and the lack of any evidence for non-subaqueous environments. By interpolation, all volcanoclastic units in the BRG are also thought to have been emplaced under water. This is confirmed by diagnostic evidence within the volcanoclastic rocks themselves for some units or areas, such as turbidite or argillite interbeds (D'Alembert tuff, Stadacona member, Jévis Sud unit) and chilled margins on volcanic fragments (Monsabrais area, Tannahill Township area, *lac* Duparquet area, *lac* Labyrinthe area).

We are unaware of observations of wave reworking in the volcanoclastic deposits, suggesting that deposition took place below the water depth affected by storm waves ( $\geq 200$  m; e.g., Mueller et al. 1994). Further constraints on water depth cannot be given for the emplacement of volcanoclastic rocks, since the traditionally held view that magma vesiculation is suppressed at depths of several kilometres due to extreme hydrostatic pressures has been rendered invalid by the discoveries of vesicular juvenile fragments and vesicular coherent lavas in deep oceans during recent investigations (e.g., Clague et al. 2003 and references therein). Magma vesicularity in submarine eruptions is a function of ocean depth, but also of juvenile gas contents and other variables.

### Nomenclature

Naming of all volcanoclastic rocks follows the system proposed by White and Houghton (2006) and references therein. Note that “hyaloclastite” in the widest accepted sense designates volcanoclastic rocks formed by all types of fragmentation of moving lava flows under water, including subaqueous autobrecciation, and that the clasts do not necessarily have to be glassy (White and Houghton 2006). Therefore, pillow breccia is a type of hyaloclastite, and so is “flow-top breccia” (e.g., Ayres 1982) lacking pillows or pillow fragments.

For Archean volcanic rocks having experienced metamorphism and in some cases hydrothermal alteration, magmatic affinities cannot be consistently

determined using major elements. Therefore, ratios of immobile trace elements such as Zr/Y, La/Yb or Th/Yb are used to assign magmatic affinities (Ross and Bédard 2009). ‘Transitional’ is employed to describe rocks which plot between tholeiitic and calc-alkaline fields.

### D'Alembert tuff

#### Host succession

The D'Alembert tuff (informal name) belongs to a sequence of folded, mostly steeply dipping, BRG volcanic rocks composed dominantly of intermediate to mafic, massive to pillowed lavas (Fig. 2). These rocks were assigned to the Renault-Dufresnoy Formation by one of us (J.G.) in 1995 (MRNF geological maps, scale 1:20 000; see also Goutier 1997). The petrography and geochemistry of the lavas near the D'Alembert tuff are discussed by Ross et al. (2008b).

#### Overall characteristics of the D'Alembert tuff

The D'Alembert tuff is a bedded volcanoclastic unit which extends about 12.5 km from Baie D'Alembert in *lac* Duparquet to just east of Highway 101 according to provincial survey maps (Fig. 2). Two main outcrop areas, A2 and A3, expose thick, coarse volcanoclastic beds. Thinner, finer-grained beds are exposed on the shores of *baie* D'Alembert (area A1) (Ross et al. 2007) and are intersected in diamond drill cores from the Baie D'Alembert showing area (Ross 2010). We infer, in agreement with previous workers (Dimroth and Demarcke 1978; Tassé et al. 1978), that areas A2 and A3 are more proximal to the vent(s) than area A1 (Ross et al. 2007, 2008b).

The exposed stratigraphic thickness of the D'Alembert tuff is approximately 300 m (Dimroth and Demarcke 1978), whereas the minimum total stratigraphic thickness reaches 545 m to 820 m. Despite the folding of the sequence, penetrative deformation remains minor in the volcanoclastic rocks, especially for the lapilli-tuffs and tuff-breccias.

A lens of lava is intercalated in the D'Alembert tuff south of area A2. It consists of pillow basalts overlain by rhyolite breccias interpreted as an extrusive dome or thick lava flow (Ross et al. 2008b). The rhyolite unit has been dated by U-Pb methods, as reported in the companion paper (Ross et al. 2010), showing that the D'Alembert tuff belongs to the youngest volcanic rocks in the BRG. Small intervals of pillow lava also exist south of area A3 (Fig. 2 and see Tassé et al. 1978). Base metal mineralization is found in at least two areas along the northern contact of the D'Alembert tuff; the western occurrence is known as the Baie D'Alembert showing (Ross 2010).

### **Known characteristics of the volcanoclastic strata in proximal areas**

Tassé et al. (1978) prepared stratigraphic sections of the D'Alembert tuff in areas A2 and A3, which they referred to as "D'Alembert" and "Reneault", respectively. Detailed work on what were then good-quality outcrops allowed Tassé et al. (1978) to classify volcanoclastic beds into two types, according to their grain-sizes, structures and thicknesses. Type "a" beds are thicker (mean of 2.75 m), coarser-grained (mostly tuff-breccias), and often do not display internal stratification. Most of these beds are massive, with only normal or reverse grading, or both. Type "b" beds are thinner (mean thickness of 0.5 m), finer-grained (lapilli-tuffs and tuffs), and most include a stratified division above the massive division. The maximum bed thickness is about 30 m and several clasts over 1 m in size were reported (Tassé *in* Dimroth et al. 1974). Tassé et al. (1978) stated that in volcanoclastic rocks from area A2, "sorting is better, mean clast smaller, bedding better defined and primary structures better organized" than in rocks from A3.

Dimroth and Demarcke (1978) performed detailed petrography on volcanoclastic samples from the same stratigraphic sections. They made a clear distinction between rocks from area A2 and those from area A3. The former contain abundant "pumice and bubble wall shards" (average of 48% in point counts), as well as plagioclase crystals and crystal fragments (average 26%); these two components were interpreted as juvenile. The "pumice" (i.e., scoria, since the clasts are not felsic) contains 60-70% vesicles and large (1-7 mm) stubby, lath-shaped plagioclase phenocrysts and glomero-phenocrysts. A wide array of volcanic lithic fragments, interpreted as non-juvenile, complete the componentry of A2 volcanoclastic rocks (average 24%).

Rocks from area A3, in contrast, do not contain "pumice" or many free crystals; they are essentially monomictic with >95% of clasts consisting of "plagioclase phyric basaltic andesite" fragments with an average of 12% vesicles (chemical composition was estimated as "basaltic andesite" by Dimroth and Demarcke 1978 based on the optical mineralogy). These clasts contain similar plagioclase crystals to those of the "pumice" from area A2 and were interpreted as the juvenile component in area A3. Two other important observations made by Dimroth and Demarcke (1978) were that the deposits are not welded, which means they were emplaced cold, and that particles clearly derived from pillow lavas are absent.

### **Existing geochemical knowledge**

A regional study in the D'Alembert tuff identified two geochemical types: a common low-Ti variety and a much rarer high-Ti variety (Ross et al. 2008b). So many geochemical differences exist between the two types that Ross et al. (2008b) suggested that they represent petrogenetically distinct batches of magma. No consistent field or petrographic differences were noted, however, between the two geochemical types, and the rare high-Ti samples did not seem to occur at specific stratigraphic positions. Since two of the three high-Ti samples identified by Ross et al. (2008b) occurred in area A3, it was decided to re-log and sample one of Tassé et al.'s (1978) stratigraphic sections in this area, to clarify the chemostratigraphy of the D'Alembert tuff and to determine whether the interpretation of emplacement processes could be improved.

### **Stratigraphic section in the D'Alembert tuff**

The updated section in area A3 – corresponding approximately with Tassé et al.'s Reneault-E section – displays 227 m of near-vertical volcanoclastic stratigraphy, including many unexposed intervals, plus 11 m of gabbro at the top (Fig. 3).

#### *Bed thickness and structures*

If interpreting the vertical continuity of beds under unexposed areas based on grain size patterns is allowed, then the thickest bed is at least 24 m-thick in the stratigraphic section. For completely exposed beds, none is thinner than 3.2 m and the average thickness is 8.2 m. Out of 27 at least partly exposed beds, 16 display normal grading, 12 have reverse grading at the base, and only 3 have diffuse internal stratification at the top (e.g., Fig. 4a). When a bed top is fine-grained, wide, shallow channels, inferred to have been excavated during passage of the next density currents, are sometimes seen (Fig. 4a). Typically, such basal erosional surfaces are overlain by a thick, coarse-grained deposit with reverse grading at its base.

#### *Clast sizes, shapes, and composition*

The largest measured clast in the stratigraphic section, found at ~200.5 m, is 60 cm long on a horizontal plane (Fig. 4b). Rare vertical outcrops reveal that the long axis of most clasts is sub-vertical, but the clasts are not strongly elongated. The shape of large clasts varies in the stratigraphic section, ranging overall from sub-rounded to angular. From 165 m upwards, the largest clasts are typically angular to sub-angular (Fig. 4b), and in some beds something approaching a jigsaw-fit texture is seen (Fig. 4c). The large fragments are not in contact with each other since they are separated by smaller clasts, but judging from their shapes, they were formerly in contact and came from a larger domain of cooled magma. Brittle



failure of this domain of cooled magma created the large clasts, which subsequently moved a few cm to dm from each other, during transport.

The large volcanic clasts are intermediate to mafic in appearance and are typically plagioclase-phyric (e.g., Fig. 5a). In the stratigraphic section, the clast vesicularity is difficult to judge on outcrops, but a few tens of meters to the east on a typical glacially polished outcrop, quartz amygdales represent 10-20% of the clasts (Fig. 5b). No felsic clasts were noted in the field.

#### *Geochemistry*

With 13 new samples positioned as regularly as possible over 227 m of volcanoclastic stratigraphy (Fig. 3, red triangles), it was hoped that a temporal evolution in the geochemical composition of the D'Alembert tuff would be documented. In particular, we hoped to find again the rare high-Ti samples of previous studies. Figure 6, Table 1 and Table 2 show that all the new samples have a similar composition to one another and fall within, or only slightly extend, the previously defined low-Ti fields. None fall in the high-Ti fields. This geochemical homogeneity in volcanoclastic samples suggests that the magma which erupted to produce beds found in the stratigraphic section was itself quite homogeneous, and that juvenile clasts were not severely contaminated by non-juvenile materials. This homogeneity of volcanoclastic rocks in area A3 was also recognized petrographically by Dimroth and Demarcke (1978), who noted the presence of only 0-3% "dacite" fragments (composition from optical mineralogy).

#### **Origin of the D'Alembert tuff**

##### *Transport and depositional processes for proximal areas*

Volcanoclastic beds from areas A2 and A3 are poorly sorted, somewhat lenticular in nature, and some have erosive bases, demonstrating emplacement of particles from laterally moving currents. The deposits are not welded and so were emplaced cool, from the passage of aqueous density currents. The clast concentration in these currents likely varied from high to low, and the turbulence from low to high, resulting in different grain support mechanisms in the currents, different depositional processes, and different deposits.

The thickest, coarsest beds, which often lack a stratified division (type "a" of Tassé et al. 1978), are very common in the relogged stratigraphic section from area A3 and were clearly produced by high-concentration density currents. These beds have some similarity to the deposits of the "gravelly high-density turbidity currents" of Lowe (1982), specifically his divisions R<sub>2</sub> (inversely graded traction carpet deposit) and R<sub>3</sub> (normally graded suspension deposit). Note

that although Lowe (1982) calls these gravelly flows "turbidity currents", the role of turbulence is limited in the depositional zone of such flows due to high particle concentration and large grain size (Fisher 1984; Lowe 1988). Tassé et al. (1978) proposed that their type "a" beds were deposited by suspension from laminar flows or "debris flows", at least for the most proximal occurrences. The flows could have become more turbulent away from the source (e.g., Lajoie and Stix 1992), becoming high concentration turbidity currents.

Finer-grained deposits (the tops of some type "a" beds, and whole type "b" beds) could then be the result of "sandy high-density turbidity currents" which are produced when the gravel-sized fragments have already been deposited up-flow (Lowe 1982). Eventually these can become low-density turbidites which develop lamination and cross-bedding, as seen in many type "b" beds.

##### *Source of the fragments*

In areas A2 and A3, the succession consists of numerous volcanoclastic beds, without intercalated sedimentary deposits or lava flows, suggesting relatively quick emplacement in density currents and a consistent abundance of volcanic debris. An abundant source of scoriaceous clasts and free plagioclase crystals is needed for the beds in area A2, and the most likely source is one or several large and vigorous submarine explosive eruption column(s) created from disintegration of a plagioclase-phyric, vesiculated magma (more discussion on the eruptive setting below). Following their introduction into the ocean, the fragments were either (1) directly entrained in debris flows and turbidity currents (eruption-fed aqueous density currents of White 2000), for example due to eruption column collapse; or (2) temporarily deposited on the seafloor and then remobilized in density currents. It is not possible to definitely exclude the second option since the proposed final transport and deposition mechanisms are identical in the two options, but we prefer eruption-fed aqueous density currents, as in the model of Fiske and Matsuda (1964). Note that these submarine debris flows are not pyroclastic flows *sensu stricto* (White 2000) since gas is not the interstitial medium between fragments in the flows.

For area A3, the transport and deposition mechanisms envisaged are the same, but the origin of the fragments likely differs. Instead of scoriaceous clasts and free crystals, the deposits contain abundant porphyritic, weakly vesicular juvenile fragments of homogenous composition. Dimroth and Demarcke (1978) proposed that these fragments were derived from the "collapse or localized explosion of andesite domes and spines" which had already crystallized at

the time of the eruption. This is compatible with our interpretation that the porphyritic clasts in the logged stratigraphic section formed by brittle failure and came from a larger domain of cooled magma and separated slightly during transport.

According to Dimroth and Demarcke (1978), rocks from area A3 do not have equivalents elsewhere in the D'Alembert tuff, whereas the scoria-bearing samples from area A2 are more representative of the entire D'Alembert tuff. Therefore, the general model for the D'Alembert tuff remains an origin by explosive eruptions of a vesiculated magma, and the clasts of area A3, which formed by collapse of a cooled, poorly vesicular dome or spine, represent a local variant.

#### *Eruptive setting*

Previous workers suggested that the D'Alembert tuff was deposited under water but that the density currents originated onland as pyroclastic flows (Dimroth and Demarcke 1978; Tassé et al. 1978). The idea that the explosive eruptions could have taken place under water was not mentioned, presumably because at the time, hydrostatic pressure was widely thought to completely suppress explosivity beyond a certain ocean depth (e.g., Fisher 1984). It is now known that explosive eruptions are possible and not uncommon at water depths of 1 km or more (e.g., Gill et al. 1990; Clague et al. 2003; Head and Wilson 2003; White et al. 2003; Allen and McPhie 2009). There is no evidence for subaerial eruptive conditions in the entire BRG or within older volcanic rocks of the Abitibi Subprovince. We thus suppose that the explosive eruptions which generated the D'Alembert tuff took place under water.

### **Monsabrais area**

#### **Host succession**

The rocks of the BRG centered on *lac* Monsabrais consist of mafic to intermediate, transitional to calc-alkaline coherent submarine lavas (massive to pillowed) and volcanoclastic rocks, cross-cut by diorites, gabbros, and the synvolcanic Monsabrais Pluton (Ross et al., 2008a; Fig. 7). The Monsabrais Pluton is a multiphase intrusion ranging in composition from tonalite to quartz diorite. The volcanic rocks around *lac* Monsabrais were also assigned to the Renault-Dufresnoy Formation by Goutier et al. (2007b). This formation extends approximately to the Baie Fabie Fault, in the south, and stratigraphically overlies the Hébécourt Formation, in the north (Fig. 7).

The volcanic stratigraphy in the Monsabrais area youngs to the south in a homoclinal sequence, at least to the Baie Babie Fault. Further east around *lac* Duparquet, volcanic rocks are folded and plunging to the east. Within the homoclinal sequence, dips

decrease from sub-vertical in the north to about 40°S just south of the Monsabrais Pluton. Both the vesicularity of lava flows and the proportion of fragmental units increase southward (Sharpe and Thibault 1966a, 1966b; Dimroth et al. 1974, 1985). Various lines of evidence, including facies changes in the volcanic rocks, the pattern of mafic to intermediate dykes, and the presence of a synvolcanic pluton, can be used to suggest that the Monsabrais area represents a distinct volcanic centre (Thibault 1963; Dimroth et al. 1973, 1974, 1982; Ross et al. 2008a). Specifically, Dimroth et al. (1985) envisaged the Monsabrais volcano, now exposed in oblique cross-section, "as a shield, about 15 km in radius, erupted upon a deep lava plain [the Hébécourt Formation]".

The level of tectonic strain is extremely low in the Monsabrais area and the volcanic textures are very well preserved. Regional metamorphism reaches only sub-greenschist grade (e.g., Powell et al. 1993, 1995), with higher grades around the Monsabrais Pluton. Two Cu-Zn VMS deposits of ~0.5-1.5 Mt each, Fabie (formerly New Inesco) and Magusi (formerly Iso), are found to the south of the Baie Fabie fault (Meyers and MacLean 1983; Liaghat and MacLean 1995).

There are no rhyolites in the Monsabrais area, preventing direct dating of the volcanism by U-Pb methods. However, a tonalitic phase of the Monsabrais Pluton has been dated at ~2696 Ma (FOOTNOTE 1); this gives a minimum age for volcanic rocks of the Monsabrais area. The tholeiitic rhyolite at the top of the Hébécourt Formation, further north, has been dated at ~2702 Ma (FOOTNOTE 1), giving a maximum age for the Monsabrais volcanic rocks.

#### **Overview of volcanoclastic rocks**

Fragmental rocks of intermediate to mafic composition are fairly abundant in the Monsabrais area, although they are rarer north of the Monsabrais Pluton. Immediately south of the pluton, in areas M1 and M2, they consist mostly of monomictic lapillituffs and tuff-breccias which lack bedding or grading and are intimately intermixed with coherent subaqueous lava flows. Jigsaw-fit textures are seen locally and these rocks are interpreted as being dominantly hyaloclastite (see Ross et al. 2008a, for details and specific facies descriptions). Here we document additional volcanoclastic rocks west of the Monsabrais Pluton (area M3), and in the Baie Magusi map unit (Fig. 7).

#### **M3 volcanoclastic units**

West of the Monsabrais Pluton, fragmental deposits are exposed in a recent forestry clearing (Fig. 8). A series of outcrops together define a calc-alkaline, mafic to intermediate volcanic sequence containing

two volcanoclastic units (units 1 and 2, informal names) separated by pillow lavas. Volcanoclastic beds generally strike eastward and they dip 56° to the south on average. They young southward and are truncated by a northeast-striking gabbro on the west side, and the Monsabrais Pluton on the east side. On the south side, the contact of unit 2 with the overlying lavas can only be interpolated.

#### *Unit 1*

Unit 1 has a 110 m apparent thickness (measured horizontally) and is dominated by monomictic tuff-breccia and lapilli-tuff. Westward, unit 1 is replaced by massive lavas on the other side of a gabbro which may occupy a synvolcanic fault since unit 2 is more laterally continuous. Towards the top, unit 1 is intercalated with pillow lavas. The largest clast in unit 1 is 30 cm across; most volcanic fragments are macroscopically aphyric and amygdaloidal. Clast vesicularity is visually estimated to reach 60% and most vesicles are filled by quartz and epidote. Clast shapes range from round or even amoeboid to curvilinear (Fig. 9a). In one outcrop at least, clasts display chilled or altered margins. Often the rocks are clast-supported or nearly so. Rapid clast size changes are not observed. No geochemical analyses are available for this volcanoclastic unit.

#### *Lavas between units 1 and 2*

The macroscopically aphyric pillow lavas separating unit 1 from unit 2 have an apparent thickness of 25-42 m; the single available geochemical analysis suggests they are basaltic andesites or andesites (Figs. 10a, 10b: yellow dot). Magmatic affinity is shown to be calc-alkaline on the Zr-Y diagram (Fig. 10c) and on La-Yb and Th-Yb diagrams as well (not shown). The analysis plots within the previously defined field for area M1 on Figs. 10b and 10c.

#### *Unit 2*

Unit 2 has an apparent thickness of 208 m and its basal contact is erosive into the pillow lavas (Fig. 9b). Unit 2 contains macroscopically plagioclase-aphyric fragments – rather than macroscopically aphyric clasts – and is characterized by more abrupt grain-size changes than unit 1. Tuff beds a few cm to dm thick were observed, although the bulk of the rocks are lapilli-tuffs. Tuff-breccias represent at least a quarter of the exposed surface. The rocks range from matrix-supported to clast-supported. Plagioclase crystals in the fragments can reach 2 mm but free crystals were not documented. Fragments range from weakly to strongly amygdaloidal and some have partly angular or curvilinear shapes (Fig. 10c), whereas others appear sub-rounded. Vesicles are filled by

quartz, epidote and albite. No chilled margins were noted.

On an outcrop illustrating the contact between pillow lavas and unit 2, a strip about 2 m-wide was mapped in detail using a mosaic of ~1 m<sup>2</sup> photos (Fig. 11). The stratigraphically lower (northern) part of the outcrop consists of pillow lavas which were eroded prior to the deposition of unit 2. Erosion created a wavy contact and the upper convex parts of some pillows are missing. Volcanoclastic debris with no textural relation with the underlying lavas has been deposited in the troughs of, and from beds above, the contact. The first 2.5 m of unit 2 at this location consists of tuff and lapilli-tuff horizons displaying cross-bedding and low amplitude channels. The rest of the outcrop consists of generally coarser (lapilli-tuff to tuff-breccia), often normally graded, beds which are up to several metres thick (Fig. 11).

Volcanoclastic rocks from unit 2 (triangles on Fig. 10) are chemically indistinguishable, based on immobile trace elements, from the underlying pillow lavas, and also from lavas and volcanoclastic rocks in area M1 further east. This suggests that they are not derived from a distant, unrelated source, despite the textural differences.

#### *Younger lavas*

Unit 2 is covered by macroscopically aphyric, massive to pillowed lavas further south (Fig. 8). These have a tholeiitic to transitional affinity, and a mafic to intermediate composition (Fig. 10). Incompatible trace element abundances are lower than in the underlying calc-alkaline rocks, and multi-element plots display much flatter patterns (not shown).

#### *Interpretation of M3 volcanoclastic rocks*

Unit 1: given the lateral facies change into massive lava, the intercalation of pillow lava towards the top of the volcanoclastic unit, the monomict aspect of the volcanoclastic rocks, the absence of bedding, the nearly clast-supported texture in places, and the presence of round to amoeboid clasts, some with inferred chilled margins, the preferred interpretation for unit 1 is a fragmental lava flow (hyaloclastite).

Unit 2: this volcanoclastic unit has an erosive base and internal channels demonstrating lateral emplacement from currents. It is clear that unit 2 does not represent in situ hyaloclastite. The currents that deposited the relatively fine-grained and relatively thin beds found just above the eroded pillows were probably not capable of causing the observed erosive features. Stronger currents of the type that deposited beds several metres thick including numerous blocks, higher up in the section, could have eroded the pillows; they just did not leave a deposit at this particular location. The nature of the laterally moving

currents remains uncertain, but currents fed by explosive eruptions are possible. Another option is the remobilisation of hyaloclastite generated in the general vicinity. This second option is supported by geochemical data, since volcanoclastic rocks from unit 2 are not chemically distinguishable from the underlying lavas, suggesting a common magmatic source and limited transport. W. Mueller (pers. commun., 2009) prefers reworking by waves in a shallow-water setting to explain the traction structures seen at the base of unit 2. However, no evidence of alternating current directions (e.g., symmetrical ripples) was seen in the deposits.

### **Baie Magusi map unit**

#### *Field description*

The Baie Magusi map unit (new informal name) occurs along *rivière* Magusi, on the northwest side of *baie* Magusi and inland, and on islands in *lac* Duparquet (Fig. 7; Sharpe and Thibault 1966b). This makes it up to 1.3 km in apparent thickness (measured horizontally) and 13 km in length on the current map. Unfortunately, a combination of difficult access in some parts of the map unit and poor outcrop quality in most of the other parts makes an overall assessment of the characteristics and origin of this map unit difficult (we described only 17 outcrops in ~10 km<sup>2</sup>). The name “map unit” is utilized to show that this is not a true stratigraphic unit, as will become clear below. On the original map (Sharpe and Thibault 1966b) the volcanoclastic rocks are shown to be very frequently intercalated with, or contain bodies of, lava (incorrectly labelled as “dacite” due to a pale weathering colour). We did observe pillowed to massive lavas in the map unit. In other words, the current representation of a major volcanoclastic unit is partly misleading, since the Baie Magusi map unit actually consist of intercalated massive to pillowed lavas and volcanoclastic rocks, like the rest of the Monsabrais area, the difference being the increased abundance of volcanoclastic rocks. These volcanoclastic rocks are quite variable in character; we give two contrasting examples to illustrate this diversity.

(i) On the shores of *baie* Magusi itself, volcanoclastic rocks in which the fragments have thick (>5 mm) chilled margins and irregular to amoeboid shapes are exposed in places (e.g., Figs. 12a-b). The volcanic fragments do not look like normal sack-shaped pillows but are more elongate, as is typical of pillow-bearing flow-foot breccia in subaqueous lava deltas (Walker 1992) or of “isolated-pillow breccia” not necessarily emplaced on steep slopes and gradational downward into close-packed pillow lava (Carlisle 1963). In one *baie* Magusi example, such

volcanoclastic rocks contain tongues of lava up to several metres long (Fig. 12c).

(ii) The most common type of volcanoclastic rock in the Baie Magusi map unit is coarse (lapilli-tuff or tuff-breccia), non-stratified at the available scale of observation, and contains fragments that are white to pale grey colour in weathered surface (Figs. 12d-e). Fragments can be aphyric to plagioclase-phyric, in the same outcrop, and vesicularity ranges up to 40% (amygdales locally reach a few centimetres across). Clast shape is typically angular (blocky), sub-angular, or sub-rounded, and the clasts lack chilled margins. More rarely, clasts are irregular (almost rag-like) or amoeboid in shape, and may have thin (<2 mm) chilled margins. Irregular and angular fragments have been observed in the same square metre (e.g., Fig. 12d). These clasts do not look like classic pillow fragments, but fit the general description of “flow-top breccia” given by Ayres (1982, p. 346). Plagioclase crystals may be present or absent from the tuffaceous matrix; in some cases they are more abundant in the matrix than in the fragments.

#### *Geochemistry*

Limited geochemical data suggests different signatures in the western, central and eastern portion of the Baie Magusi map unit. Specifically, the eastern samples are basaltic andesites or andesites (Figs. 13a, 13b) with lower Zr/Y and La/Yb ratios (Figs. 13c, 13d); higher heavy REE concentrations (Fig. 13f); and flatter heavy REE patterns (Fig. 13g) relative to the other sectors. The central and western samples are more mafic and have higher Zr/Y and La/Yb. The western sample can be distinguished from the central rocks by its lower Zr/TiO<sub>2</sub>, lower Th/Yb, and steeper heavy REE slope. The lower Zr/TiO<sub>2</sub> ratio of the western sample is due both to a lesser Zr-Hf plateau and a smaller Ti anomaly. Note that the massive lava sampled 160 m NW of the northern contact of the Baie Magusi map unit in the central portion (pink dot on Fig. 13) is chemically indistinguishable from the volcanoclastic rocks sampled in the same area (orange triangles). Despite the internal geochemical variations in the Baie Magusi map unit, its overall trace element profiles resemble those found in samples taken in areas M1 and M2 (see Fig. 10 for M1 and Ross et al. 2008a for M2).

#### *Emplacement processes*

No single process or event can explain the genesis of the Baie Magusi map unit, given its internal variations and great apparent thickness. The type (i) volcanoclastic rocks described above from the shores of *baie* Magusi unambiguously represent the disintegration of a lava flow under water, probably on a slope. Unfragmented (massive to pillowed) lavas

also occur in the map unit. These two observations, together with the lack of bedding, demonstrate that lavas contributed significantly to the genesis of the rocks and that the Baie Magusi map unit is not a bedded volcanoclastic sequence of possible pyroclastic origin comparable to the D'Alembert tuff and the Stadacona member. This does not exclude the possibility that some of the volcanoclastic rocks in the Baie Magusi map unit may have been formed by explosive eruptions, but our observations indicate that the bulk of the unit was not formed this way. This conclusion is important in establishing the evolution and architecture of the BRG.

However, the genesis of the bulk of the volcanoclastic rocks in the map unit (such as the type ii rocks described above) remains uncertain. Fragmentation and rapid chilling of a number of submarine lava flows, followed by variable amounts of transport, appears to be a plausible origin. Factors that may have led to more fragmentation of lavas relative to the rest of the Monsabrais area include shallower emplacement depths (Dimroth et al. 1978) (and/or increased vesicularity) and, possibly, steeper slopes on the flanks of the Monsabrais volcano. Staudigel and Schmincke (1984) suggest that seamount growth and shoaling caused by accumulation of extrusive products and by sill emplacement creates steep fault scarps. Lava flowing on such steep slopes will tend to fragment and disaggregate.

### **Lac Duparquet**

The BRG in the *lac Duparquet* area is folded in a series of folds, the axes of which plunge to the ESE (Fig. 7). The area is dominated by submarine, mafic to intermediate, aphyric to plagioclase-phyric, variably vesicular lavas. A variety of intermediate to mafic volcanoclastic rocks are exposed, often very well, on the shores and islands of the lake, but they do not form thick or laterally widespread units (this section excludes the Baie Magusi map unit discussed in the previous section). These volcanoclastic rocks mostly originated as lava flows (e.g., pillow breccias, hyaloclastite), not as a result of explosive eruptions. Fragmental lavas alternate with pillowed and massive lavas. These four examples show the main features of the rocks:

(i) The repetitive transition between massive to pillowed lavas and pillow breccia is exposed at field station 06-PSR-174, a peninsula in the east-central portion of the lake (Fig. 14a).

(ii) A superb example of a pillow breccia was seen at station 06-PSR-189 in the northwest part of the lake, where two nearly complete elliptical pillows are surrounded by broken pillows and hyaloclastite (Fig. 14b).

(iii) Station 06-PSR-172 in the north-central portion of the lake exposes monomict, matrix- to clast-supported tuff-breccias. The aphyric, vesicular fragments are wavy, elongate (average dip of the long axis: 70° south), up to 50 cm long; they have 0.5-1 cm-thick chilled margins (Figs. 14c and 14d). Some are isolated in finer particles whereas others are grouped very closely. The grouped fragments have shapes that suggest *in situ* individualisation from larger lava domains, and an originally plastic (deformable) state. The clast marked by an arrow on figure 14d contains a dark sub-vertical band a few mm across, that looks exactly like the chilled margins of nearby clasts. A possible interpretation is that a fracture propagated through this clast but did not cross it entirely; water flowed through the fracture and caused chilling of a few mm of material on both sides. For other fragments, such as those in the lower-left part of the picture, the fracturing and chilling of the (newly formed) margins was complete and the fragments separated by a few centimetres due to continued movement of the lava flow.

(iv) Finally, station 07-PSR-133 in the west-central portion of the lake displays diffusely-layered volcanoclastic rocks containing rare exotic felsic clasts (Fig. 15). These are interpreted as remobilized hyaloclastite. Overlying the diffusely layered rocks are coarser monomictic volcanoclastic rocks in contact with a body of slightly invasive coherent lava or a subvolcanic intrusion. Most fragments in the monomictic rocks appear to be derived from the coherent body, suggesting a peperitic relationship.

### **Geological evolution of the Renault-Dufresnoy Formation west of Highway 101**

The Renault-Dufresnoy Formation between the Ontario-Québec border and Highway 101 in Québec is a package of submarine volcanic rocks which displays a consistent set of physical and chemical characteristics: mafic to intermediate compositions dominate, very few rhyolites occur, transitional to calc-alkaline affinities are dominant, macroscopic plagioclase crystals are common, the rocks are often amygdaloidal (more so than in the rest of the BRG), and volcanoclastic rocks are comparatively abundant. Most of these volcanoclastic rocks are lava flow-related (with the exception of the D'Alembert tuff). Major faults do not seem to complicate the stratigraphy and the folding pattern is simple. Therefore, this package of rocks can be considered a structural block in which we can attempt to reconstruct the volcanic architecture or at least the general evolution. The following points are the elements of the puzzle which we are confident about (Fig. 16):

1. The oldest Reneault-Dufresnoy rocks in the study area are in the Monsabrais sector, lying just above a rhyolite in the Hébécourt Formation dated at ~2702 Ma. There is no major fault between the two formations and there is no thick sedimentary unit at the contact (R. Rogers, MSc in progress at INRS), suggesting a relatively short time gap, although it is possible that a condensed section occurs there (Thurston et al. 2008).
2. The lava-dominated Reneault-Dufresnoy sequence in the Monsabrais area forms a tilted volcanic edifice as discussed above. In general, the proportion of volcanoclastic rocks increases upward in this edifice. This may be explained by progressively steeper slopes, which favour both the disintegration of flowing lava and remobilisation of volcanoclastic debris, relative to a lava plain. Also, several fragmentation processes become progressively more effective in shallower water (e.g., Staudigel and Schmincke 1984).
3. The M3 volcanoclastic rocks occur towards the middle of this Monsabrais edifice, probably on the west flank. They were eventually covered by a thick succession of lavas, prior to the intrusion of the medium-grained, equigranular Monsabrais Pluton.
4. The Baie Magusi map unit, which consists mostly of a series of massive, pillowed and fragmental lavas, sits on the eastern flank of the Monsabrais volcano, towards the top.
5. The youngest rocks in Reneault-Dufresnoy Formation (and the whole BRG), in the core of a syncline, are those of the D'Alembert tuff, which contains a rhyolite lens dated at ~2695 Ma. It seems likely that the (eruption-fed?) aqueous density currents which created the D'Alembert tuff dumped their load in a E-W subsiding basin or depression present in a pre-existing, lava-dominated volcanic edifice. The exact nature of this edifice is unclear. A depression is needed to allow preservation of these rocks (otherwise the D'Alembert tuff would be eroded); after an episode of N-S tectonic shortening, the depression became a syncline. The most proximal rocks in the D'Alembert tuff are in its eastern part (area A3), suggesting that the vent for the volcanoclastic rocks is definitely not related to the Monsabrais volcano, to the west.
6. The above points demonstrate a general younging of the Reneault-Dufresnoy Formation from west to east in the study area.

We are uncertain how the volcanism in D'Alembert tuff area, particularly the lavas underlying the D'Alembert tuff, relates to the Monsabrais volcano through *lac Duparquet*. Previous workers suggested a

distinct volcanic complex in the D'Alembert tuff area, which they named Reneault (Dimroth et al. 1982, 1985). Although the D'Alembert tuff beds were not generated by eruptions from the Monsabrais volcano and need a distinct vent, it is unclear if this vent is also responsible for the generation of the underlying lavas and therefore if a distinct Renault complex actually exists. Currently available geochemical data does not help resolve the issue. Given these uncertainties, drawing a stratigraphic correlation diagram (Fig. 16) is a difficult task, but at least some elements are in place. Future volcanological and geochemical studies in the Reneault-Dufresnoy Formation may further clarify the geological evolution of the area.

### Conclusions

In this paper, we have described and interpreted volcanoclastic rocks from three areas within the Reneault-Dufresnoy Formation in the northern part of the BRG in Québec. From west to east, these are: (1) the Monsabrais area, where a volcanic complex contains volcanoclastic rocks mainly in three sub-areas (M1 to M3) and in the Baie Magusi map unit; (2) *lac Duparquet*, where volcanoclastic rocks are rarer, thinner and more discontinuous; and (3) the D'Alembert tuff area.

At the Monsabrais volcanic complex, explosive eruptions were rare. Volcanoclastic rocks in areas M1 to M2, south of the Monsabrais Pluton, mainly represent fragmental lava flows, i.e. more or less in situ hyaloclastite; bedding and grading are extremely rare and volcanoclastic units are laterally discontinuous. In the newly described area M3, west of the pluton, unit 1 also represents in situ hyaloclastite, but unit 2 was emplaced by density currents, with the fragments generated either as hyaloclastite or by explosive eruptions. Further south, we propose that the Baie Magusi map unit is not a bedded volcanoclastic sequence of possible pyroclastic origin comparable to the D'Alembert tuff and the Stadacona member, but rather is best interpreted as a series of mafic to intermediate lava flows and related fragmental deposits produced by the interaction of moving lava with water.

The D'Alembert tuff, in the eastern part of the study area, is the manifestation of an important period of explosive eruptions involving vesiculated, plagioclase-phyric magmas. These explosive eruptions generated, directly or indirectly, aqueous density currents of variable particle concentrations which deposited most beds of the D'Alembert tuff. This bedded volcanoclastic unit extends for over 10 km laterally and has a stratigraphic thickness of several hundred metres, making it a good marker unit. The explosive eruptions were interrupted at times, allowing the emplacement of mafic to felsic lava lenses south of

areas A2 and A3, and of argillite intervals in the Baie D'Alembert showing area. Also, it appears that volcanic fragments in thick, coarse volcanoclastic beds from the relogged section in area A3 were generated by the collapse of lava domes or spines, rather than by explosion of new erupting magma. In summary, the D'Alembert tuff was not formed by a single catastrophic explosive eruption, although the bulk of the fragments it contains were generated by submarine explosive processes.

### Acknowledgements

This study was funded by the Targeted Geoscience Initiative (TGI-3) program, Abitibi project, of the Geological Survey of Canada. Field work in the Blake River Group was done in occasional collaboration with C. Dion, E. Grunsky, M. Legault, and J. Percival. We acknowledge discussions and/or correspondence with J. Bédard, H. Gibson, T. Monecke, W. Mueller, V. Pearson, P. Thurston and J.D.L. White on topics related to this study. K. Lauzière helped with drafts of geological maps. R. Kerrich and D. Wyman are thanked for useful reviews. MRNF contribution number BEGQ 8439-2010/2011-1.

### Footnotes

1. McNicoll, V., Goutier, J., Dubé, B., Mercier-Langevin, P., Ross, P.-S., Dion, C., Monecke, T., Percival, J., Legault, M., and Gibson, H., submitted. New U-Pb geochronology from the Blake River Group, Abitibi Greenstone Belt, Québec: implications for geological interpretations and base metal exploration. *Economic Geology*.

### References

- Allen, S.R., and McPhie, J. 2009. Products of neptunian eruptions. *Geology*, **37**: 639-642.
- Ayer, J., Amelin, Y., Corfu, F., Kamo, S., Ketchum, J., Kwok, K., and Trowell, N. 2002. Evaluation of the southern Abitibi greenstone belt based on U-Pb geochronology; autochthonous volcanic construction followed by plutonism, regional deformation and sedimentation. *Precambrian Research*, **115**: 63-95.
- Ayres, L.D. 1982. Pyroclastic rocks in Precambrian greenstone-belt volcanoes. In *Pyroclastic volcanism and deposits of Cenozoic intermediate to felsic volcanic islands with implications for Precambrian greenstone-belt volcanoes*. Edited by L.D. Ayres. Geological Association of Canada, Short Course Notes Volume 2, pp. 343-365.
- Carlisle, D. 1963. Pillow breccias and their aquagene tuffs, Quadra Island, British Columbia. *Journal of Geology*, **71**: 48-71.
- Chadwick, W.W., Cashman, K.V., Embley, R.W., Matsumoto, H., Dziak, R.P., de Ronde, C.E.J., Lau, T.K., Deardorff, N.D., and Merle, S.G. 2008. Direct video and hydrophone observations of submarine explosive eruptions at NW Rota-1 volcano, Mariana arc. *Journal of Geophysical Research*, **113**: article B08S10.
- Clague, D.A., Davis, A.S., and Dixon, J.E. 2003. Submarine strombolian eruptions on the Gorda Mid-Ocean ridge. In *Explosive subaqueous volcanism*. Edited by J.D.L. White, J.L. Smellie, and D.A. Clague. American Geophysical Union, Geophysical Monograph 140, pp. 111-128.
- Corfu, F. 1993. The evolution of the southern Abitibi greenstone belt in light of precise U-Pb geochronology. *Economic Geology*, **88**: 1307-1322.
- Corfu, F., Krogh, T.E., Kwok, Y.Y., and Jensen, L.S. 1989. U-Pb geochronology in the southwestern Abitibi greenstone belt, Superior Province. *Canadian Journal of Earth Sciences*, **26**: 1747-1763.
- Cousineau, P., and Dimroth, E. 1982. Interpretation of the relations between massive, pillowed and brecciated facies in an archean submarine andesite volcano -- amulet andesite, Rouyn-Noranda, Canada. *Journal of Volcanology and Geothermal Research*, **13**: 83-102.
- Couture, J.-F., and Goutier, J. 1996. Métallogénie et évolution tectonique de la région de Rouyn-Noranda. Ministère des ressources naturelles (Québec), report MB 96-06, 110 p. (<http://www.mrnf.gouv.qc.ca/english/mines/geology/geology-databases.jsp>)
- David, J., Dion, C., Goutier, J., Roy, P., Bandyayera, D., Legault, M., and Rhéaume, P. 2006. Datations U-Pb effectuées dans la Sous-province de l'Abitibi à la suite des travaux de 2004-2005. Ministère des Ressources naturelles et de la Faune (Québec), report RP 2006-04, 22 p. (<http://www.mrnf.gouv.qc.ca/english/mines/geology/geology-databases.jsp>)
- Dimroth, E. 1977. Archean subaqueous autoclastic volcanic rocks, Rouyn-Noranda area, Quebec: classification, diagnosis and interpretation. *Geological Survey of Canada, Current Research*, **77-1A**: 513-522. (<http://geopub.nrcan.gc.ca/>)
- Dimroth, E., and Demarcke, J. 1978. Petrography and mechanism of eruption of the Archean D'Alembert tuff, Rouyn-Noranda, Quebec, Canada. *Canadian Journal of Earth Sciences*, **15**: 1712-1723.
- Dimroth, E., Boivin, P., Goulet, N., and Larouche, M. 1973. Tectonic and volcanological studies in the Rouyn-Noranda area. Ministère des richesses naturelles (Québec), report DP 138, 60 p. (<http://www.mrnf.gouv.qc.ca/english/mines/geology/geology-databases.jsp>)
- Dimroth, E., Côté, R., Provost, G., Rocheleau, M., Tassé, N., and Trudel, P. 1974. Third progress report on the stratigraphy, volcanology, sedimentology and structure of Rouyn-Noranda area, counties of Rouyn-Noranda, Abitibi-west and Temiskamingue. Ministère des Richesses naturelles (Québec), report DP 300, 64 p. (<http://www.mrnf.gouv.qc.ca/english/mines/geology/geology-databases.jsp>)



- Dimroth, E., Cousineau, P., Leduc, M., and Sanschagrin, Y. 1978. Structure and organisation of Archean subaqueous basalt flows, Rouyn-Noranda area, Quebec, Canada. *Canadian Journal of Earth Sciences*, **15**: 902-918.
- Dimroth, E., Imreh, L., Rocheleau, M., and Goulet, N. 1982. Evolution of the south-central part of the Archean Abitibi belt, Quebec. Part I: stratigraphy and paleogeographic model. *Canadian Journal of Earth Sciences*, **19**: 1729-1758.
- Dimroth, E., Imreh, L., Cousineau, P., Leduc, M., and Sanschagrin, Y. 1985. Paleogeographic analysis of mafic submarine flows and its use in the exploration for massive sulphide deposits. *In* Evolution of Archean Supracrustal sequences. *Edited by* L.D. Ayres, P.C. Thurston, K.D. Card and W. Weber. Geological Association of Canada, Special Paper **28**, pp. 203-222.
- Dubé, B., Mercier-Langevin, P., Hannington, M., Lafrance, B., Gosselin, G., and Gosselin, P. 2007. The LaRonde Penna world-class Au-rich volcanogenic massive sulfide deposit, Abitibi, Québec: mineralogy and geochemistry of alteration and implications for genesis and exploration. *Economic Geology*, **102**: 633-666.
- Fisher, R.V. 1984. Submarine volcanoclastic rocks. *In* Marginal basin geology. *Edited by* B.P. Kokelaar and M.F. Howells. Geological Society of London, Special Publication 16, pp. 5-27.
- Fiske, R.S., and Matsuda, T. 1964. Submarine equivalents of ash flows in the Tokiwa Formation, Japan. *American Journal of Science*, **262**: 76-106.
- Franklin, J.M., Gibson, H.L., Jonasson, I.R., and Galley, A.G. 2005. Volcanogenic massive sulfide deposits. *Economic Geology*, 100<sup>th</sup> Anniversary Volume: 523-560.
- Galley, A.G. 2003. Composite synvolcanic intrusions associated with Precambrian VMS-related hydrothermal systems. *Mineralium Deposita*, **38**: 443-473.
- Galley, A.G., and van Breemen, O. 2002. Timing of synvolcanic magmatism in relation to base-metal mineralization, Rouyn-Noranda, Abitibi volcanic belt, Quebec. *Geological Survey of Canada, Current Research*, **2002-F8**: 1-9. (<http://geopub.nrcan.gc.ca/>)
- Gélinas, L., Trudel, P., and Hubert, C. 1984. Chemostratigraphic division of the Blake River Group, Rouyn-Noranda area, Abitibi, Quebec. *Canadian Journal of Earth Sciences*, **21**: 220-231.
- Gibson, H.L., and Watkinson, D.H. 1990. Volcanogenic massive sulphide deposits of the Noranda Cauldron and shield volcano, Quebec. *In* The northwestern Quebec polymetallic belt: a summary of 60 years of mining exploration. *Edited by* M. Rive, P. Verpaelt, Y. Gagnon, J.-M. Lulin, G. Riverin and A. Simard, CIM Special Volume 43, pp. 119-132.
- Gibson, H., and Galley, A. 2007. Volcanogenic massive sulphide deposits of the Archean, Noranda district, Quebec. *In* Mineral deposits of Canada: a synthesis of major deposit types, district metallogeny, the evolution of geological provinces, and exploration methods. *Edited by* W.D. Goodfellow. Geological Association of Canada, Mineral Deposits Division, Special Publication 5, pp. 533-552.
- Gill, J., Torssander, P., Lapierre, H., Taylor, R., Kaiho, K., Koyama, M., Kusakabe, M., Aitchison, J., Cisowski, S., Dadey, K., Fujioka, K., Klaus, A., Lovell, M., Marsaglia, K., Pezard, P., Taylor, B., and Tazaki, K. 1990. Explosive deep water basalt in the Sumisu backarc rift. *Science*, **248**: 1214-1217.
- Goodwin, A.M. 1977. Archean volcanism in Superior Province, Canadian Shield. *In* Volcanic regimes in Canada. *Edited by* W.R.A. Baragar, L.C. Coleman and J.M. Hall. Geological Association of Canada, Special Paper 16, pp. 205-241.
- Goodwin, A.M. 1982. Archean volcanoes in southwestern Abitibi belt, Ontario and Quebec: form, composition, and development. *Canadian Journal of Earth Sciences*, **19**: 1140-1155.
- Goutier, J. 1997. Géologie de la région de Destor (SNRC 32D/07). Ministère des ressources naturelles (Québec), report RG 96-13, 37 p. (<http://www.mrnf.gouv.qc.ca/english/mines/geology/geology-databases.jsp>)
- Goutier, J., Monecke, T., Ross, P.-S., and Dion, C. 2007a. Volcanoclastites du Groupe de Blake River et implications pour les SMV. Ministère des Ressources naturelles et de la Faune, Québec, report GM 63072, 22 p. (<http://www.mrnf.gouv.qc.ca/english/mines/geology/geology-databases.jsp>)
- Goutier, J., Dion, C., Legault, M., Ross, P.-S., McNicoll, V., de Kemp, E., Percival, J., Monecke, T., Bellefleur, G., Mercier-Langevin, P., Lauzière, K., Thurston, P., and Ayer, J. 2007b. Units in the Blake River Group: correlations, geometry and mineral potential. Québec Exploration 2007, Abstracts of oral presentations and posters. Ministère des Ressources naturelles et de la Faune (Québec), report DV 2007-05, p. 99.
- Goutier, J., McNicoll, V.J., Dion, C., Lafrance, B., Legault, M., Ross, P.-S., Mercier-Langevin, P., Cheng, L.-Z., de Kemp, E., and Ayer, J. 2009. L'impact du Plan cuivre et de l'IGC-3 sur la géologie de l'Abitibi et du Groupe de Blake River. Ministère des Ressources naturelles et de la Faune (Québec), report GM 64195, p. 9-13. (<http://www.mrnf.gouv.qc.ca/english/mines/geology/geology-databases.jsp>)
- Hannington, M.D., Santaguida, F., Kjarsgaard, I.M., and Cathles, L.M. 2003. Regional-scale hydrothermal alteration in the Central Blake River Group, western Abitibi subprovince, Canada: implications for VMS prospectivity. *Mineralium Deposita*, **38**: 393-422.
- Head, J.W., and Wilson, L. 2003. Deep submarine pyroclastic eruptions: theory and predicted landforms and deposits. *Journal of Volcanology and Geothermal Research*, **121**: 155-193.
- Hudak, G.J., Morton, R.L., Franklin, J.M., and Peterson, D.M. 2003. Morphology, distribution, and



- estimated eruption volumes for intracaldera tuffs associated with volcanic-hosted massive sulfide deposits in the Archean Sturgeon Lake Caldera Complex, northwestern Ontario. *In Explosive Subaqueous Volcanism. Edited by J.D.L. White, J.L. Smellie and D.A. Clague.* American Geophysical Union, Geophysical Monograph 140, pp. 345-360.
- Jensen, L.S., and Langford, F.F. 1985. Geology and petrogenesis of the Archean Abitibi belt in the Kirkland Lake area, Ontario. Ontario Geological Survey, Miscellaneous Paper 123, 130 p. (<http://www.geologyontario.mndmf.gov.on.ca/>)
- Kerr, D.J., and Gibson, H.L. 1993. A comparison of the Horne volcanogenic massive sulfide deposit and intracauldron deposits of the Mine Sequence, Noranda, Quebec. *Economic Geology*, **88**: 1419-1442.
- Laflèche, M.R., Dupuy, C., and Dostal, J. 1992. Tholeiitic volcanic rocks of the late Archean Blake River Group, southern Abitibi greenstone belt: origin and geodynamic implications. *Canadian Journal of Earth Sciences*, **29**: 1448-1458.
- Lafrance, B., Davis, D.W., Goutier, J., Moorhead, J., Pilote, P., Mercier-Langevin, P., Dubé, B., Galley, A.G., and Mueller, W.U., 2005. Nouvelles datations isotopiques dans la portion québécoise du Groupe de Blake River et des unités adjacentes. Ministère des ressources naturelles et de la faune (Québec), report RP 2005-01, 15 p. (<http://www.mrnf.gouv.qc.ca/english/mines/geology/geology-databases.jsp>)
- Lajoie, J., and Stix, J. 1992. Volcaniclastic rocks. *In Facies models - response to sea level change. Edited by R.G. Walker and N.P. James.* Geological Association of Canada, Geotext 1, pp. 101-119.
- Legault, M., Goutier, J., Beaudoin, G. and Aucoin, M. 2005. Synthèse métallogénique de la Faille de Porcupine-Destor, Sous-province de l'Abitibi. Ministère des Ressources naturelles et de la Faune (Québec), report ET 2005-01, 35 p.
- Liaghat, S., and MacLean, W.H. 1995. Lithochemistry of altered rocks at the New Inco VMS deposit, Noranda, Quebec. *Journal of Geochemical Exploration*, **52**: 333-350.
- Lowe, D.R. 1982. Sediment gravity flows: II. Depositional models with special reference to the deposits of high-density turbidity currents. *Journal of Sedimentary Petrology*, **52**: 279-297.
- Lowe, D.R. 1988. Suspended-load fallout rate as an independent variable in the analysis of current structures. *Sedimentology*, **35**: 765-776.
- Mercier-Langevin, P., Dubé, B., Hannington, M.D., Davis, D.W., Lafrance, B., and Gosselin, G. 2007a. The LaRonde Penna Au-rich volcanogenic massive sulfide deposit, Abitibi Greenstone Belt, Quebec: part I. geology and geochronology: *Economic Geology*, **102**: 585-609.
- Mercier-Langevin, P., Dubé, B., Hannington, M.D., Richer-Lafleche, M., and Gosselin, G. 2007b. The LaRonde Penna Au-rich volcanogenic massive sulfide deposit, Abitibi Greenstone Belt, Quebec: part II. lithochemistry and paleotectonic setting: *Economic Geology*, **102**: 611-631.
- Mercier-Langevin, P., Ross, P.-S., Lafrance, B., and Dubé, B. 2008. Volcaniclastic rocks of the Bousquet scoriaceous tuff units north of the LaRonde Penna mine, Doyon-Bousquet-LaRonde mining camp, Abitibi Greenstone Belt, Quebec. *Geological Survey of Canada, Current Research*, **2008-11**: 1-19. (<http://geopub.nrcan.gc.ca/>)
- Meyers, R.E., and MacLean, W.H. 1983. The geology of the New Inco copper deposit, Noranda district, Quebec. *Canadian Journal of Earth Sciences*, **20**: 1291-1304.
- Montelius, C., Allen, R.L., Svenson, S.-Å., and Weihed, P. 2007. Facies architecture of the Palaeoproterozoic VMS-bearing Mauriliden volcanic centre, Skellefte district, Sweden. *Journal of the Geological Society of Sweden (GFF)*, **129**: 177-196.
- Mortensen, J. K. 1993. U-Pb geochronology of the eastern Abitibi Subprovince. Part 2: Noranda -Kirkland Lake area. *Canadian Journal of Earth Sciences*, **30**: p. 29-41.
- Mueller, W. 2006. A new interpretation of the Blake River Group, Abitibi greenstone belt: the importance of volcanological facies mapping and the discovery of a megacaldera; *Ashfall*, **62**: 10-13.
- Mueller, W., Chown, E.H., and Potvin, R. 1994. Substorm wave base felsic hydroclastic deposits in the Archean Lac des Vents volcanic complex, Abitibi belt, Canada. *Journal of Volcanology and Geothermal Research*, **60**: 273-300.
- Paradis, S., Ludden, J., and Gélinas, L. 1988. Evidence for contrasting compositional spectra in comagmatic intrusive and extrusive rocks of the late Archean Blake River Group, Abitibi, Quebec. *Canadian Journal of Earth Sciences*, **25**: 134-144.
- Pearson, V., and Daigneault, R. 2009. An Archean megacaldera complex: the Blake River Group, Abitibi greenstone belt. *Precambrian Research*, **168**: 66-82.
- Péloquin, A.S., Potvin, R., Paradis, S., Laflèche, M.R., Verpaelst, P., and Gibson, H.L. 1990. The Blake River Group, Rouyn-Noranda area, Quebec: a stratigraphic synthesis. *In The northwestern Quebec polymetallic belt: a summary of 60 years of mining exploration. Edited by M. Rive, P. Verpaelst, Y. Gagnon, J.-M. Lulin, G. Riverin and A. Simard, CIM Special Volume 43*, pp. 107-118.
- Péloquin, A.S., Piercey, S.J., and Hamilton, M.A. 2008. The Ben Nevis volcanic complex, Ontario, Canada: part of the late volcanic phase of the Blake River Group, Abitibi Subprovince. *Economic Geology*, **103**: 1219-1241.
- Piercey, S.J., Chaloux, E.C., Pelouquin, A.S., Hamilton, M.A., and Creaser, R.A. 2008. Synvolcanic and younger plutonic rocks from the Blake River Group: implications for regional metallogenesis. *Economic Geology*, **103**: 1243-1268.
- Powell, W.G., Carmichael, C.J., and Hodgson, C.J. 1993. Thermobarometry in a subgreenschist to greenschist transition in metabasites of the Abitibi

- greenstone belt, Superior Province, Canada. *Journal of Metamorphic Geology*, **11**: 165-178.
- Powell, W.G., Carmichael, D.M., and Hodgson, C.J. 1995. Condition and timing of metamorphism in the southern Abitibi greenstone belt, Quebec. *Canadian Journal of Earth Sciences*, **21**: 787-805.
- Ross, P.-S. 2010. The Baie D'Alembert showing, an example of base metal mineralization in mafic lavas and volcanoclastic rocks of the Blake River Group, Abitibi Greenstone Belt, Quebec. Geological Survey of Canada, Current Research, **2010-6**: 1-12 (<http://geopub.nrcan.gc.ca/>)
- Ross, P.-S., and Bédard, J.H. 2009. Magmatic affinity of modern and ancient subalkaline volcanic rocks determined from trace-element discriminant diagrams. *Canadian Journal of Earth Sciences*, **46**: 823-839.
- Ross, P.-S., Percival, J.A., Mercier-Langevin, P., Goutier, J., McNicoll, V.J., and Dubé, B. 2007. Intermediate to mafic volcanoclastic units in the peripheral Blake River Group, Abitibi Greenstone Belt, Quebec: origin and implications for volcanogenic massive sulphide exploration. Geological Survey of Canada, Current Research, **2007-C3**: 1-25. (<http://geopub.nrcan.gc.ca/>)
- Ross, P.-S., Goutier, J., McNicoll, V.J., and Dubé, B. 2008a. Volcanology and geochemistry of the Monsabrais area, Blake River Group, Abitibi Greenstone Belt, Quebec: implications for volcanogenic massive sulphide exploration. *Current Research* **2008-1**: 1-18. (<http://geopub.nrcan.gc.ca/>)
- Ross, P.-S., Goutier, J., Percival, J.A., Mercier-Langevin, P., and Dubé, B. 2008b. New volcanological and geochemical observations from the Blake River Group, Abitibi Greenstone Belt, Quebec: the D'Alembert tuff, the Stadacona unit, and surrounding lavas. Geological Survey of Canada, Current Research, **2008-17**: 1-27. (<http://geopub.nrcan.gc.ca/>)
- Ross, P.-S., Goutier, J., Legault, M., Grunsky, E., and Dubé, B., 2009. New volcanological and geochemical observations from the Blake River Group, Abitibi Greenstone Belt, Ontario and Quebec: Tannahill Township and Lake Labyrinth: Geological Survey of Canada, Current Research, **2009-8**: 1-26. (<http://geopub.nrcan.gc.ca/>)
- Ross, P.-S., McNicoll, V., Goutier, J., Mercier-Langevin, P., and Dubé, B. 2010. Basaltic to andesitic volcanoclastic rocks in the Blake River Group, Abitibi Greenstone Belt: 2. Origin, geochemistry, and geochronology. *Canadian Journal of Earth Sciences*, **X**: XX-XXX.
- Sharpe, J.I. and Thibault, C. 1966a. Quartz sud-ouest du canton de Hébécourt, comté d'Abitibi-Ouest. Ministère des Richesses naturelles (Québec), geological map, scale 1:12 000 (<http://www.mrnf.gouv.qc.ca/english/mines/geology/geology-databases.jsp>)
- Sharpe, J.I. and Thibault, C. 1966b. Quartz sud-est du canton de Hébécourt, comté d'Abitibi-Ouest. Ministère des Richesses naturelles (Québec), geological map, scale 1:12 000 (<http://www.mrnf.gouv.qc.ca/english/mines/geology/geology-databases.jsp>)
- Spence, C.D., and de Rosen-Spence, A.F. 1975. The place of sulfide mineralization in the volcanic sequence at Noranda, Quebec. *Economic Geology*, **70**: 90-101.
- Staudigel, H., and Schmincke, H.-U. 1984. The Pliocene seamount series of La Palma/Canary Islands. *Journal of Geophysical Research*, **89**: 11,195-11,215.
- Sun, S.-S., and McDonough, W.F. 1989. Chemical and isotopic systematics of oceanic basalts: implications for mantle composition and processes. *In* Magmatism in the ocean basins. Edited by A.D. Saunders and M.J. Norry. Geological Society of London, Special Publication 42, pp. 313-345.
- Tassé, N., Lajoie, J., and Dimroth, E. 1978. The anatomy and interpretation of an Archean volcanoclastic sequence, Noranda region, Quebec. *Canadian Journal of Earth Sciences*, **15**: 874-888.
- Thibault, C. 1963. Rapport préliminaire sur la moitié sud du canton d'Hébécourt, comté d'Abitibi-Ouest. Ministère des Richesses naturelles (Québec), report DP 090, 30 p. (<http://www.mrnf.gouv.qc.ca/english/mines/geology/geology-databases.jsp>)
- Thurston, P.C., Ayer, J.A., Goutier, J., and Hamilton, M.A. 2008. Depositional gaps in Abitibi Greenstone Belt stratigraphy: a key to exploration for syngenetic mineralization. *Economic Geology*, **103**: 1097-1134.
- Walker, G.P.L. 1992. Morphometric study of pillow-size spectrum among pillow lavas. *Bulletin of Volcanology*, **54**: 459-474.
- White, J.D.L. 2000. Subaqueous eruption-fed density currents and their deposits. *Precambrian Research*, **101**: 87-109.
- White, J.D.L., and Houghton, B.F. 2006. Primary volcanoclastic rocks. *Geology*, **34**: 677-680.
- White, J.D.L., Smellie, J.L., and Clague, D.A. 2003. Introduction: a deductive outline and topical overview of subaqueous explosive volcanism. *In* Explosive Subaqueous Volcanism. Edited by J.D.L. White, J.L. Smellie and D.A. Clague. American Geophysical Union, Geophysical Monograph 140, pp. 1-23.
- Winchester, J.A., and Floyd, P.A. 1977. Geochemical discrimination of different magma series and their differentiation products using immobile elements. *Chemical Geology*, **20**: 325-343.

Table 1. Major element data (in weight percent) and quality control results for the samples plotted in figures 6, 10 and 13.

Sample number	Easting	Northing	Short rock description	SiO <sub>2</sub>	TiO <sub>2</sub>	Al <sub>2</sub> O <sub>3</sub>	Fe <sub>2</sub> O <sub>3</sub>	FeO	MnO	MgO	CaO	Na <sub>2</sub> O	K <sub>2</sub> O	P <sub>2</sub> O <sub>5</sub>	Cr <sub>2</sub> O <sub>3</sub>	LOI	Tot
<i>Activation Laboratories Ltd., Ancaster, Ontario (fusion XRF or fusion ICP-AES)</i>																	
<b>D'Alembert tuff, section in area A3</b>																	
BR-282	642296	5368188	Tuff	59.32	0.56	17.52	5.19	n.d.	0.068	2.97	6.40	1.70	1.89	0.11	n.d.	3.28	99.0
BR-283	642298	5368171	Tuff-breccia	62.65	0.50	16.75	4.67	n.d.	0.062	2.85	4.63	5.29	0.27	0.10	n.d.	2.64	100.4
BR-284	642320	5368166	Tuff-breccia	62.44	0.50	16.44	4.69	n.d.	0.064	2.87	5.90	3.41	0.72	0.10	n.d.	2.76	99.9
BR-285	642322	5368147	Tuff	59.89	0.51	17.29	5.09	n.d.	0.067	3.31	7.23	2.25	1.22	0.11	n.d.	3.65	100.6
BR-286	642324	5368132	Tuff	58.89	0.53	18.50	5.14	n.d.	0.068	3.53	6.77	2.79	1.02	0.10	n.d.	3.63	101.0
BR-287	642325	5368121	Tuff	57.82	0.55	18.38	5.34	n.d.	0.059	3.57	5.87	2.37	1.61	0.10	n.d.	3.75	99.4
BR-288	642327	5368106	Lapilli tuff	58.79	0.53	16.53	5.37	n.d.	0.065	3.64	7.08	2.35	0.77	0.10	n.d.	3.47	98.7
BR-289	642329	5368084	Tuff	59.68	0.55	17.44	5.32	n.d.	0.082	3.36	7.63	1.96	1.23	0.12	n.d.	3.54	100.9
BR-291	642332	5368055	Lapilli tuff	59.65	0.52	17.62	5.09	n.d.	0.066	3.20	7.77	2.17	1.13	0.10	n.d.	3.53	100.8
BR-292	642334	5368044	Lapilli tuff	59.40	0.51	17.54	5.16	n.d.	0.067	3.30	7.34	1.90	1.34	0.10	n.d.	3.19	99.9
BR-294	642337	5368015	Tuff	57.04	0.60	17.82	6.07	n.d.	0.081	3.93	7.83	2.16	0.94	0.13	n.d.	3.57	100.2
BR-295	642339	5368002	Tuff	56.30	0.62	17.61	6.25	n.d.	0.090	4.12	7.17	2.21	1.25	0.14	n.d.	3.73	99.5
BR-296	642340	5367988	Lapilli tuff	57.75	0.63	17.08	6.29	n.d.	0.089	4.13	7.79	2.44	0.81	0.15	n.d.	3.73	100.9
<b>Monsabrais area M3</b>																	
BR-268	614169	5369337	Lapilli tuff	54.18	0.66	17.52	3.35	3.66	0.112	5.03	8.47	3.54	0.67	0.11	< 0.01	2.61	100.3
BR-269	614232	5369520	Lapilli tuff	52.13	0.69	17.60	2.82	4.40	0.134	5.24	7.89	1.73	2.73	0.11	< 0.01	3.64	99.6
<b>Baie Magusi map unit</b>																	
BR-049a	615562	5366227	Lapilli-tuff	50.25	0.98	15.63	1.02	7.15	0.118	9.39	6.11	2.73	0.15	0.17	0.03	5.2	99.7
BR-226	618988	5367823	Fragmental	49.50	0.68	17.47	1.23	6.49	0.209	5.17	9.26	2.37	0.94	0.11	< 0.01	5.49	99.7
BR-227	618563	5367843	Tuff-breccia to lapilli-tuff	50.63	0.69	17.24	0.89	5.98	0.140	5.34	8.27	2.07	0.81	0.11	< 0.01	5.03	97.7
BR-228	624004	5369973	Lapilli-tuff	53.69	0.84	16.42	1.49	6.11	0.119	3.96	9.61	1.51	0.75	0.13	< 0.01	4.49	99.8
BR-256	625762	5370008	Tuff or lapilli tuff	52.38	0.72	15.40	0.69	5.87	0.094	3.99	6.91	3.36	1.23	0.11	< 0.01	8.16	99.6
BR-257	623074	5368972	Lapilli-tuff	58.27	0.71	14.59	1.64	5.09	0.108	3.77	8.53	1.89	0.18	0.10	< 0.01	3.99	99.4
BR-258	622896	5369219	Lapilli-tuff	55.72	0.77	16.38	2.95	4.78	0.094	5.18	4.50	4.60	0.27	0.12	< 0.01	4.07	100.0
BR-225	619358	5368162	Massive lava	52.35	0.69	15.86	1.60	5.75	0.136	7.82	8.51	2.96	0.65	0.12	0.02	2.92	100.0
<b>Detection limits</b>																	
For all Actlabs samples except BR-049a				0.01	0.01	0.01	0.01	0.01	0.001	0.01	0.01	0.01	0.01	0.01	0.01	0.01	n.a.
<b>Standards</b> (selected examples from year 2008: applies to D'Alembert tuff analyses)																	
DNC-1 Meas				46.85	0.49	18.4	9.85	n.d.	0.146	10.12	11.33	1.92	0.18	0.11	n.d.	n.d.	n.d.
DNC-1 Cert				47	0.48	18.3	9.93	n.d.	0.149	10.1	11.3	1.87	0.23	0.09	n.d.	n.d.	n.d.
W-2a Meas				52.31	1.08	15.31	10.87	n.d.	0.171	6.41	11.08	2.14	0.55	0.14	n.d.	n.d.	n.d.
W-2a Cert				52.4	1.06	15.4	10.7	n.d.	0.163	6.37	10.9	2.14	0.63	0.13	n.d.	n.d.	n.d.
BIR-1a Meas				47.66	0.98	15.54	11.33	n.d.	0.17	9.67	13.34	1.81	0.01	0.04	n.d.	n.d.	n.d.
BIR-1a Cert				47.8	0.96	15.4	11.3	n.d.	0.171	9.68	13.2	1.75	0.03	0.05	n.d.	n.d.	n.d.
<b>Duplicates of the presented data</b>																	
BR-286 Dup				n.d.	n.d.	n.d.	n.d.	n.d.	n.d.	n.d.	n.d.	n.d.	n.d.	n.d.	n.d.	n.d.	n.d.
<i>Acme Analytical Laboratories Ltd., Vancouver, British Columbia (fusion ICP-AES)</i>																	
<b>Monsabrais area M3</b>																	
2007043753	614276	5369372	Ultramafic intrus	42.66	0.54	9.99	12.76	n.d.	0.18	18.96	8.24	0.19	0.04	0.04	0.2	6.1	99.9
2007043771	614250	5369430	Lapilli-tuff (unit 2)	52.47	0.63	17.85	7.63	n.d.	0.11	5.30	7.31	4.92	0.82	0.09	0.017	2.8	99.9
2007043764	614120	5369061	Pillow lava	55.75	0.83	16.21	6.58	n.d.	0.09	2.43	6.62	4.37	0.95	0.07	0.046	6.0	99.9
2007043760	613851	5369003	Massive lava	44.46	0.89	15.21	12.23	n.d.	0.21	8.42	11.01	2.12	0.14	0.08	0.07	5.1	99.9
2007043758	614001	5369084	Pillow lava	52.41	1.05	19.21	8.19	n.d.	0.12	3.66	6.92	4.91	< 0.04	0.10	0.058	3.3	99.9
2007043765	614270	5369548	Pillow lava	56.84	0.60	16.76	5.91	n.d.	0.11	3.33	10.67	3.14	0.19	0.09	0.033	2.3	100.0
<b>Detection limits</b>																	
For all Acme samples				0.01	0.01	0.01	0.04	n.a.	0.01	0.01	0.01	0.01	0.01	0.01	0.002	0.1	n.a.

FeO by titration; Fe<sub>2</sub>O<sub>3</sub> is total iron where FeO is not reported.

UTM coordinates: NAD 83, zone 17.

n.a., not applicable; n.d., no data.

Actlabs data was obtained in 2006, 2007 and 2008. Acme data was obtained in 2007.

Table 2. Selected trace element data from fusion ICP-MS analyses (in ppm) and quality control results for the samples plotted in figures 6, 10 and 13.

Sample number	Ce	Dy	Er	Eu	Gd	Hf	La	Lu	Nb	Nd	Pr	Sm	Ta	Tb	Th	Y	Yb	Zr
<i>Activation Laboratories Ltd., Ancaster, Ontario</i>																		
<b>D'Alembert tuff, section in area A3</b>																		
BR-282	22.2	2.36	1.45	0.847	2.50	2.7	11.5	0.190	3.9	11.0	2.82	2.53	0.30	0.41	1.17	13.9	1.31	108
BR-283	20.9	2.12	1.28	0.690	2.29	2.5	10.9	0.178	3.4	10.3	2.64	2.38	0.36	0.37	1.08	12.5	1.21	100
BR-284	20.1	2.11	1.34	0.670	2.22	2.6	10.6	0.174	3.3	9.9	2.55	2.28	0.29	0.36	1.10	12.1	1.18	100
BR-285	20.7	2.17	1.32	0.688	2.39	2.7	9.9	0.186	3.5	9.7	2.40	2.27	0.29	0.38	1.14	12.8	1.26	105
BR-286	21.0	2.21	1.36	0.766	2.43	2.6	11.0	0.186	3.5	10.5	2.67	2.49	0.29	0.39	1.10	12.9	1.31	103
BR-287	23.2	2.40	1.48	0.798	2.56	3.0	11.2	0.203	3.8	10.6	2.69	2.47	0.33	0.41	1.30	13.8	1.38	117
BR-288	20.5	2.12	1.29	0.714	2.31	2.8	10.7	0.178	3.5	10.2	2.65	2.34	0.30	0.37	1.13	12.3	1.21	106
BR-289	21.2	2.25	1.36	0.743	2.34	2.7	11.1	0.187	3.7	10.4	2.66	2.48	0.29	0.38	1.21	13.1	1.33	111
BR-291	20.9	2.19	1.36	0.714	2.35	2.7	10.0	0.192	3.4	9.5	2.42	2.21	0.30	0.38	1.16	12.8	1.28	106
BR-292	20.6	2.16	1.33	0.682	2.32	2.7	9.9	0.187	3.4	9.3	2.38	2.20	0.29	0.37	1.18	12.7	1.23	106
BR-294	23.1	2.64	1.64	0.797	2.87	2.8	10.7	0.229	4.4	11.0	2.79	2.65	0.34	0.46	1.12	15.5	1.55	115
BR-295	24.8	2.76	1.70	0.827	2.96	2.8	11.5	0.237	4.5	11.7	2.96	2.77	0.34	0.48	1.10	16.2	1.60	112
BR-296	22.0	2.67	1.65	0.852	2.82	2.8	11.1	0.229	4.4	11.8	2.90	2.80	0.31	0.44	1.03	15.6	1.59	108
<b>Monsabrais area M3</b>																		
BR-268	22.1	2.29	1.42	0.781	2.53	2.2	10.4	0.208	3.7	10.0	2.73	2.30	0.29	0.39	1.35	13.3	1.34	83
BR-269	21.4	2.30	1.41	0.807	2.43	2.2	9.8	0.204	4.0	9.6	2.62	2.17	0.32	0.39	1.33	13.7	1.34	83
<b>Baie Magusi map unit</b>																		
BR-049a	23.7	2.7	1.6	1.0	3	2.2	9.8	0.21	4	13.2	3.04	2.9	0.3	0.5	0.9	15	1.4	84
BR-226	21.1	2.27	1.37	0.757	2.39	2.3	10.0	0.198	3.1	9.3	2.62	2.21	0.28	0.41	1.38	13.4	1.31	84
BR-227	22.8	2.44	1.48	0.757	2.71	2.5	10.5	0.217	4.2	10.0	2.79	2.32	0.45	0.44	1.43	14.0	1.40	94
BR-228	28.1	3.93	2.50	0.975	3.87	3.2	12.5	0.371	4.6	13.1	3.56	3.26	0.40	0.68	1.68	23.9	2.55	120
BR-256	23.9	2.97	1.92	0.726	2.80	2.6	10.6	0.303	3.6	11.2	3.02	2.59	0.33	0.49	1.37	18.4	1.89	97
BR-257	24.0	3.52	2.28	0.920	3.36	2.9	10.7	0.343	4.1	11.6	3.08	2.94	0.37	0.60	1.63	22.1	2.20	109
BR-258	22.8	3.25	2.05	0.886	3.21	2.6	9.7	0.310	3.8	11.5	2.96	2.77	0.32	0.56	1.33	20.7	2.05	98
BR-225	22.6	2.22	1.39	0.820	2.55	2.1	9.9	0.188	3.2	10.7	2.88	2.46	0.27	0.40	1.08	13.3	1.31	79
<b>Detection limits</b>																		
For all Actlabs samples e)	0.05	0.01	0.01	0.005	0.01	0.1	0.05	0.002	0.2	0.05	0.01	0.01	0.01	0.01	0.05	0.5	0.01	1
<b>Standards</b> (selected examples from year 2008: applies to D'Alembert tuff analyses)																		
DNC-1 Meas	8.46	2.75	1.98	0.624	2.03	1.1	3.93	0.297	1.2	4.84	1.14	1.43	0.08	0.44	0.24	17.9	2.01	39
DNC-1 Cert	10.6	2.7	2	0.59	2	1.01	3.8	0.32	3	4.9	1.3	1.38	0.098	0.41	0.2	18	2.01	41
W-2a Meas	23.3	3.72	2.29	1.15	n.d.	2.5	11.2	0.293	6.5	12.4	n.d.	3.3	0.48	0.67	2.07	21.7	2.04	95
W-2a Cert	23	3.6	2.5	1	n.d.	2.6	10	0.33	7.9	13	n.d.	3.3	0.5	0.63	2.4	24	2.1	94
BIR-1a Meas	2.11	2.47	1.71	0.532	1.79	0.6	0.8	0.237	0.3	2.33	0.39	1.08	0.03	0.4	<0.05	15.4	1.59	16
BIR-1a Cert	1.95	2.5	1.7	0.54	1.85	0.6	0.62	0.26	0.6	2.5	0.38	1.1	0.04	0.36	0.03	16	1.65	16
<b>Duplicates of the presented data</b>																		
BR-286 Dup	21.1	2.23	1.37	0.775	2.44	2.7	10.9	0.19	3.5	10.7	2.72	2.48	0.29	0.39	1.11	12.9	1.3	104
<i>Acme Analytical Laboratories Ltd., Vancouver, British Columbia</i>																		
<b>Monsabrais area M3</b>																		
2007043753	5.3	1.01	0.7	0.39	1.02	0.6	2.4	0.14	2.3	3.6	0.83	0.8	0.1	0.24	0.3	7.4	0.65	20.7
2007043771	17.5	1.78	1.2	0.65	1.93	2.5	8.4	0.2	3.8	9.4	2.28	1.85	0.2	0.39	1.4	13.3	1.14	85.6
2007043764	8.5	2.37	1.6	0.6	2.26	1.4	3.5	0.25	2.6	6.5	1.34	1.85	0.1	0.48	0.3	17.4	1.51	48.5
2007043760	7.7	1.76	1.15	0.63	1.7	1	3.3	0.2	3.4	5.7	1.2	1.37	0.2	0.37	0.5	12.3	1.2	33.4
2007043758	10.3	2.91	1.82	0.78	2.73	1.9	4.4	0.3	3.3	7.3	1.63	2.17	0.2	0.59	0.3	20.2	1.84	60.7
2007043765	17.5	1.9	1.13	0.7	2.06	2.2	8.4	0.2	3.8	10	2.34	2	0.3	0.42	1.1	13.4	1.14	83
<b>Detection limits</b>																		
For all Acme samples	0.1	0.05	0.03	0.02	0.05	0.1	0.1	0.01	0.1	0.3	0.02	0.05	0.1	0.01	0.2	0.1	0.05	0.1

## Figures

Fig. 1. (a) Map of eastern Canada showing the location of the Abitibi Greenstone Belt. (b) Simplified geological map of the Abitibi Subprovince and part of the Pontiac Subprovince, after Legault et al. (2005). (c) Simplified geological map of a portion of the Abitibi and Pontiac subprovinces showing selected VMS mines and the distribution of mafic to intermediate volcanoclastic rocks in the BRG (Québec side only, since the information has not been compiled in Ontario). Grid on all maps is UTM Nad 83, zone 17.

Fig. 2. Geologic map of the BRG in the area containing the D'Alembert tuff. The trace of the new stratigraphic section in area A3 is indicated. The position of the geochronological sample in the intercalated rhyolite is also shown (see Ross et al. 2010). Geology based on a 1 : 20,000 map (NTS 32D/06) by Ministère des Ressources naturelles et de la Faune, Québec.

Fig. 3. New stratigraphic section in area A3 of the D'Alembert tuff, drawn horizontally since beds are vertical (see inset map and Fig. 2 for location). The "0 m" stratigraphic height is arbitrary since volcanoclastic rocks continue to the north of it (not logged); they also continue beyond the southern end of the section. The grain size (for the horizontal scale) was determined by averaging the measured long axis of the five largest clasts at multiple positions for each bed. All beds are volcanoclastic (except for the gabbro at the top of the section), with clast sizes and shapes representative of field observations.

Fig. 4. Field photos of the D'Alembert tuff in the stratigraphic section (see Fig. 3 for references to heights in meters on the section). (a) Contact (dashed line) between the upper, laminated, tuffaceous part of a bed with the lower, reversely graded, lapilli-tuff to tuff-breccia part of another bed, at 195 m. (b) Close-up view on the coarsest, non-graded part of a 13 m-thick bed at 199 m and up. Note the poor sorting and the angular shapes of the large clasts, including the largest in the section. (c) A >6 m-thick bed (top not exposed), the middle part of which contains >75% blocks (angular clasts >64 mm across), at 166 m. A line drawing of the clearest features is provided to compensate for the lichen cover on the photo. The bed is reversely graded at the base and normally graded at the top. Note the near jigsaw-fit aspect of the illustrated middle portion.

Fig. 5. Field photos of the D'Alembert tuff in the stratigraphic section and nearby (see Fig. 3 for references to heights in meters on the section). (a) Close-up view of the texture of a single volcanic clast from a lapilli-tuff or tuff-breccia bed, in fresh surface with added moisture, at 108 m in the section. Note the abundance of plagioclase phenocrysts and mafic minerals in a finer groundmass. (b) Close-up view of a weathered sub-vertical surface at field station 06-PSR-017 (see Appendix) showing non-spherical quartz amygdales in a volcanic fragment.

Fig. 6. Geochemistry of the D'Alembert tuff in the stratigraphic section (red triangles and profiles) and elsewhere (fields for 20 low-Ti samples and 3 high-Ti samples). (a)-(b) Classification diagrams from Winchester and Floyd (1977). (c)-(d) Magmatic affinity diagrams from Ross and Bédard (2009). (e) TiO<sub>2</sub>-Zr diagram. (f) La-Sm diagram. (g) Multi-element diagram, showing the least mobile elements only. Primitive mantle normalisation values from Sun and McDonough (1989). The field for low-Ti samples in (g) excludes three samples which have slightly different profiles due to hydrothermal alteration or primary variation.

Fig. 7. Simplified geology near lakes Hébécourt, Monsabrais and Duparquet, showing the distribution of the senior author's field stations. Geology based on 1 : 20,000 maps (NTS 32D/06, 32D/11) by Ministère des Ressources naturelles et de la Faune, Québec. Areas M1 to M3 around *lac* Monsabrais are also shown. Source of geochronological information: see FOOTNOTE 1.

Fig. 8. Geological map of part of a new forestry clearing just west of the Monsabrais Pluton (area M3). See text for description of the geology. The western tip of the Monsabrais Pluton lies just east of this figure (location: see Fig. 7). Outcrop cleaning and mapping by the second author (Goutier et al. 2007). A third geochemical sample of lava south of unit 2 (shown in Fig. 10) lies 145 m to the WSW of the SW corner of the map.

Fig. 9. Photographs illustrating aspects of the M3 volcanoclastic rocks (location: see Figs. 8 and 11). (a) View of a tuff-breccia or lapilli-tuff in unit 1 showing curvilinear to round, pale, vesicular clasts, in a brown matrix (weathered surface; station 07-PSR-169). (b) Contact between partly eroded pillow lava (bottom of photo) and the overlying

lapilli-tuff and tuff beds from unit 2. Note the cross-bedding in the fine-grained volcanoclastic rocks. (c) Curvilinear clast (under pencil) from unit 2. Photos (b)-(c) from field station 07-PSR-170.

Fig. 10. Geochemistry of volcanoclastic rocks and one lava from area M3 (data points) compared to those from area M1 (fields) (location of samples: see Fig. 8). Also shown are three samples of lavas in the southern Fig. 8 and beyond and a sample of an olivine gabbro intrusion. (a)-(b) Classification diagrams from Winchester and Floyd (1977). (c) Magmatic affinity diagram from Ross and Bédard (2009). (d) Multi-element profiles (normalisation values from Sun and McDonough 1989).

Fig. 11. Photo-mosaic and geological map of part of an outcrop in area M3 (station 07-PSR-170 or 07-JG-5537). Tape measures are laterally spaced by 1.0 m on the photos. See text for explanation and Fig. 8 for location.

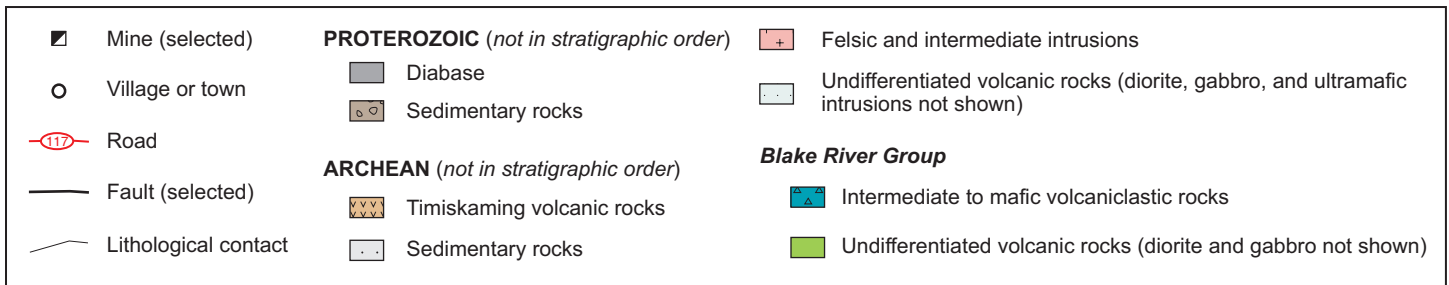
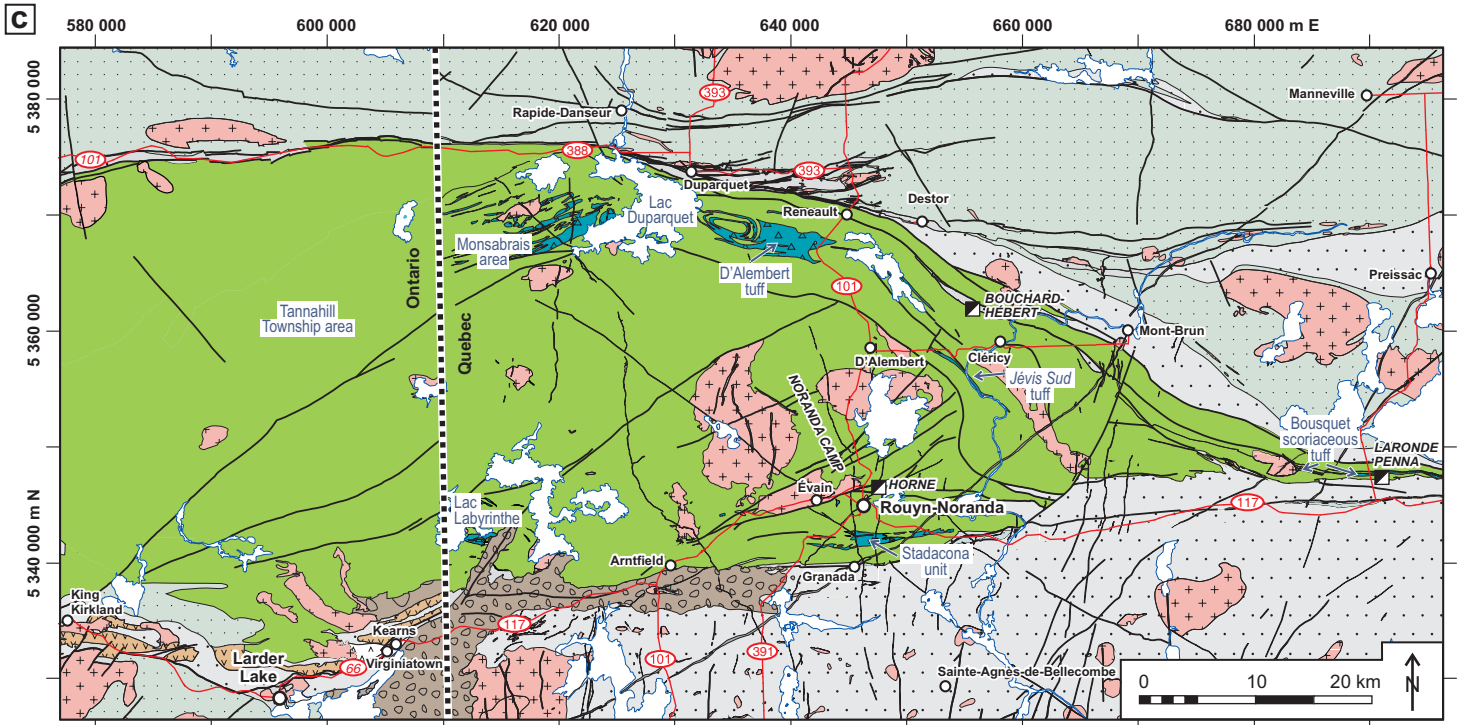
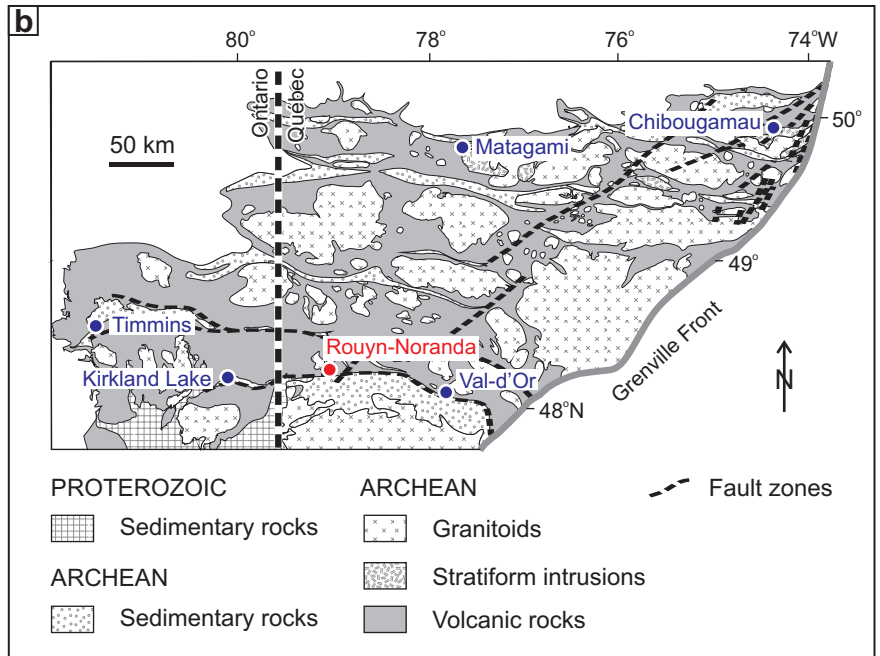
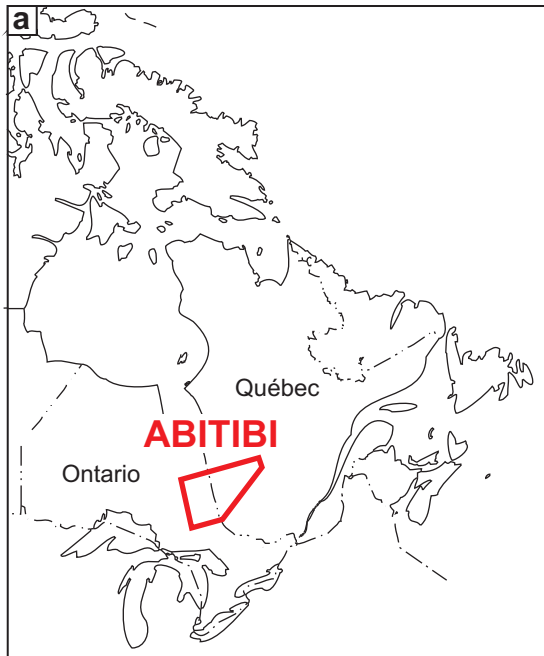
Fig. 12. Photographs of the rocks outcropping on the shore of *baie* Magusi (a-c) and from the Baie Magusi map unit elsewhere (d-e) (location: see Fig. 7). (a) Coarse volcanoclastic rock with amoeboid fragments and lava pods, with chilled margins, in an inferred hyaloclastite matrix, from the northwest corner of *baie* Magusi. (b)-(c) Other parts of the same outcrop showing lava tongues up to a few metres in length. Some of these lava pods and tongues have broken up into smaller pods and amoeboid clasts like those seen in (a), early enough in their cooling history to develop chilled margins [a-c are oblique views of a sub-horizontal outcrop at station 07-PSR-138; superimposed white to very pale green spots and black domains are lichen patches and lake scum, respectively; notebook is 20.5 cm long]. (d) Clast-supported, block-bearing coarse lapilli-tuff from the same map unit, about 4 km to the west-southwest. Notice the very irregular shape of the volcanic clast just right of the pen tip and the large vesicles partly filled by quartz in the lower-right corner. The green colour of the material around the clasts is due to a carbonate-epidote cement (station 07-PSR-067). (e) Another block-bearing coarse lapilli-tuff from a minor volcanoclastic unit just to the northwest of the Baie Magusi map unit, showing a white clast with partly curvilinear shape (station 07-PSR-070). Similar clasts are found in the Baie Magusi map unit.

Fig. 13. Geochemistry of the Baie Magusi map unit and one nearby lava. (a)-(b) Classification diagrams from Winchester and Floyd (1977). (c)-(e) Magmatic affinity diagrams from Ross and Bédard (2009). (f) Multi-element profiles. (g) Chondrite-normalised La/Sm versus Gd/Yb. Normalisation values for (f)-(g) from Sun and McDonough (1989).

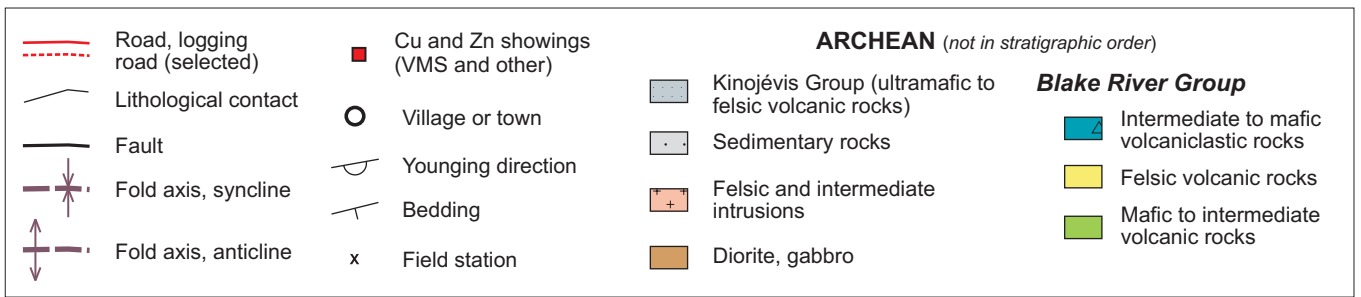
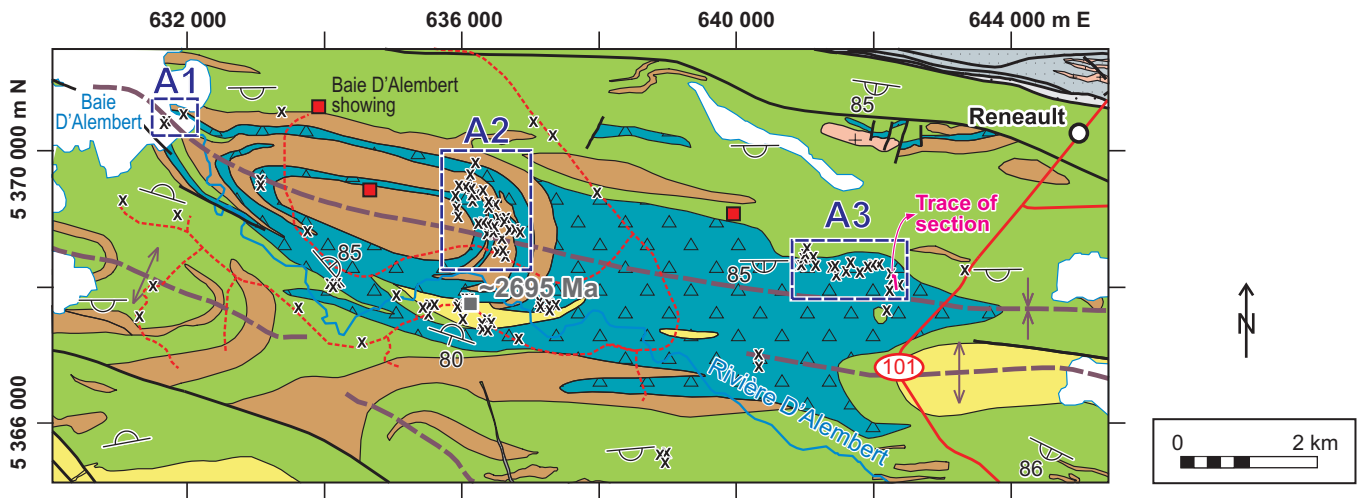
Fig. 14. Photos and field sketches of volcanoclastic rocks from the BRG in the *lac* Duparquet area (location: see Fig. 7). (a) Massive lava, pillow lava and pillow breccia at station 06-PSR-174, a gently eastward dipping outcrop. Pillows are aphyric and vesicles are often chlorite-filled. The matrix of the pillow breccia consists mostly of chloritized glass shards. (b) Flattish outcrop showing nearly complete, elliptical pillows surrounded by broken pillows and hyaloclastite (station 06-PSR-189). Notebook is 20.5 cm long. (c) Vertical rock face on island 79 (station 06-PSR-172); see text for discussion. (d) Close-up view of (c), showing isolated lava fragments with chilled margins in a hyaloclastite matrix.

Fig. 15. Photo-mosaic and geological map of the best-exposed sub-horizontal part of a peninsula on an island from *lac* Duparquet (station 07-PSR-133; location: see Fig. 7). Beds dip to the northeast at low angles. The numbers on the right side of the figure corresponds to arbitrary metres on the tape measure. See text for explanation.

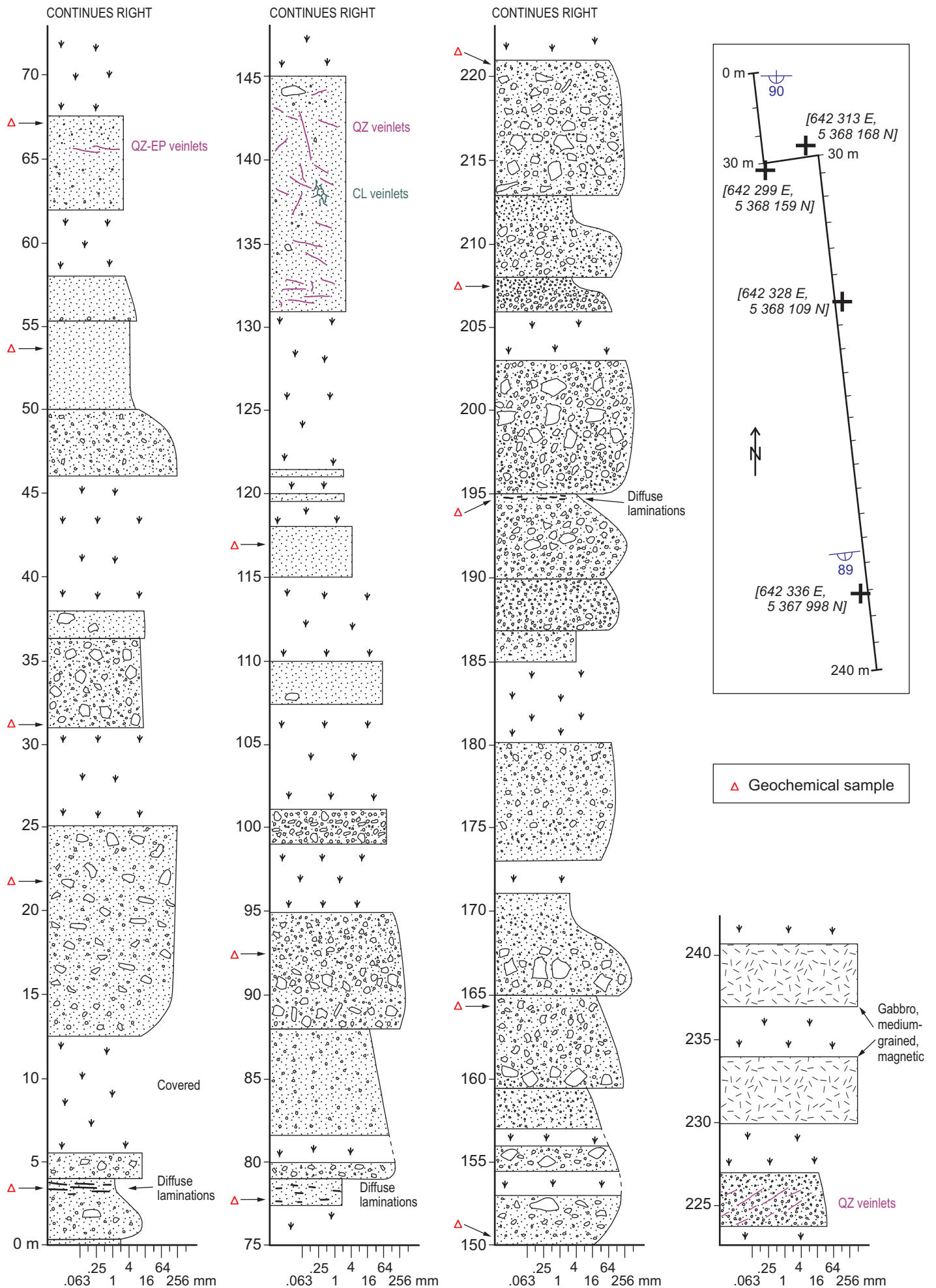
Fig. 16. Geological reconstruction of the Renault-Dufresnoy Formation between the Québec-Ontario border and Highway 101 in Québec. (a) Schematic stratigraphic sections in the Monsabrais, *lac* Duparquet and D'Alambert tuff areas. The vertical scale shows true thickness, but without the removal of mafic to intermediate intrusions. The total stratigraphic thickness of the Renault-Dufresnoy Formation implied by this reconstruction is over 6 km, but since the whole area is at lower greenschist metamorphic grade, the formation must not represent a layer cake-like pile as implied in this view. (b) Schematic vertical E-W section representing a possible pre-deformation architecture for this area, not to scale. This shows that primary dips were not horizontal and that the volcanic rocks accumulated both vertically and laterally. Volcanoclastic rocks in area M3 are in the centre of the Monsabrais volcano, whereas the Baie Magusi map unit is on the east flank, towards the top. The D'Alambert tuff is the youngest unit in the BRG, as shown by U-Pb geochronology.



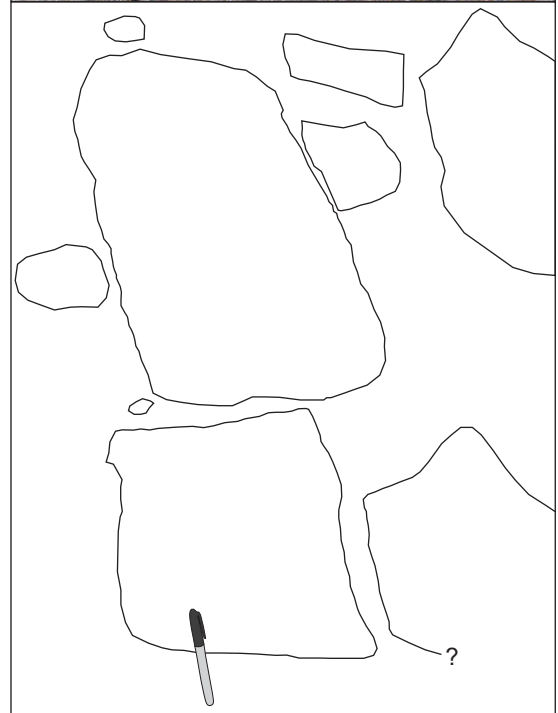
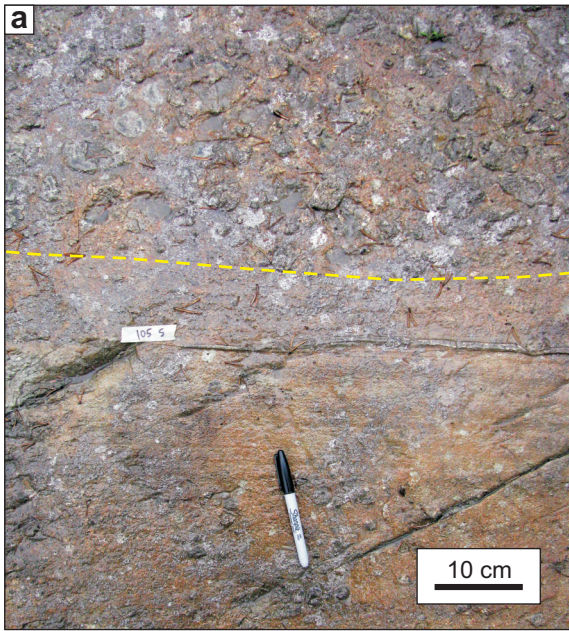




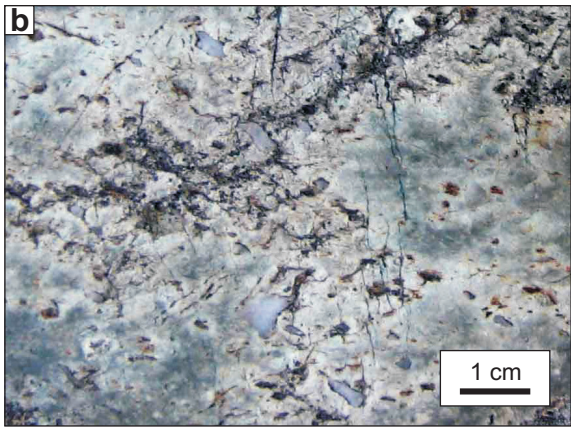
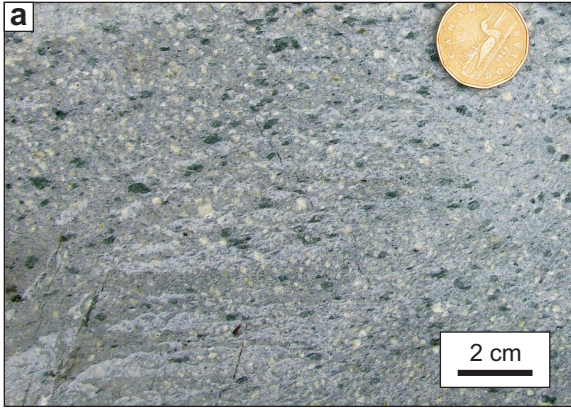


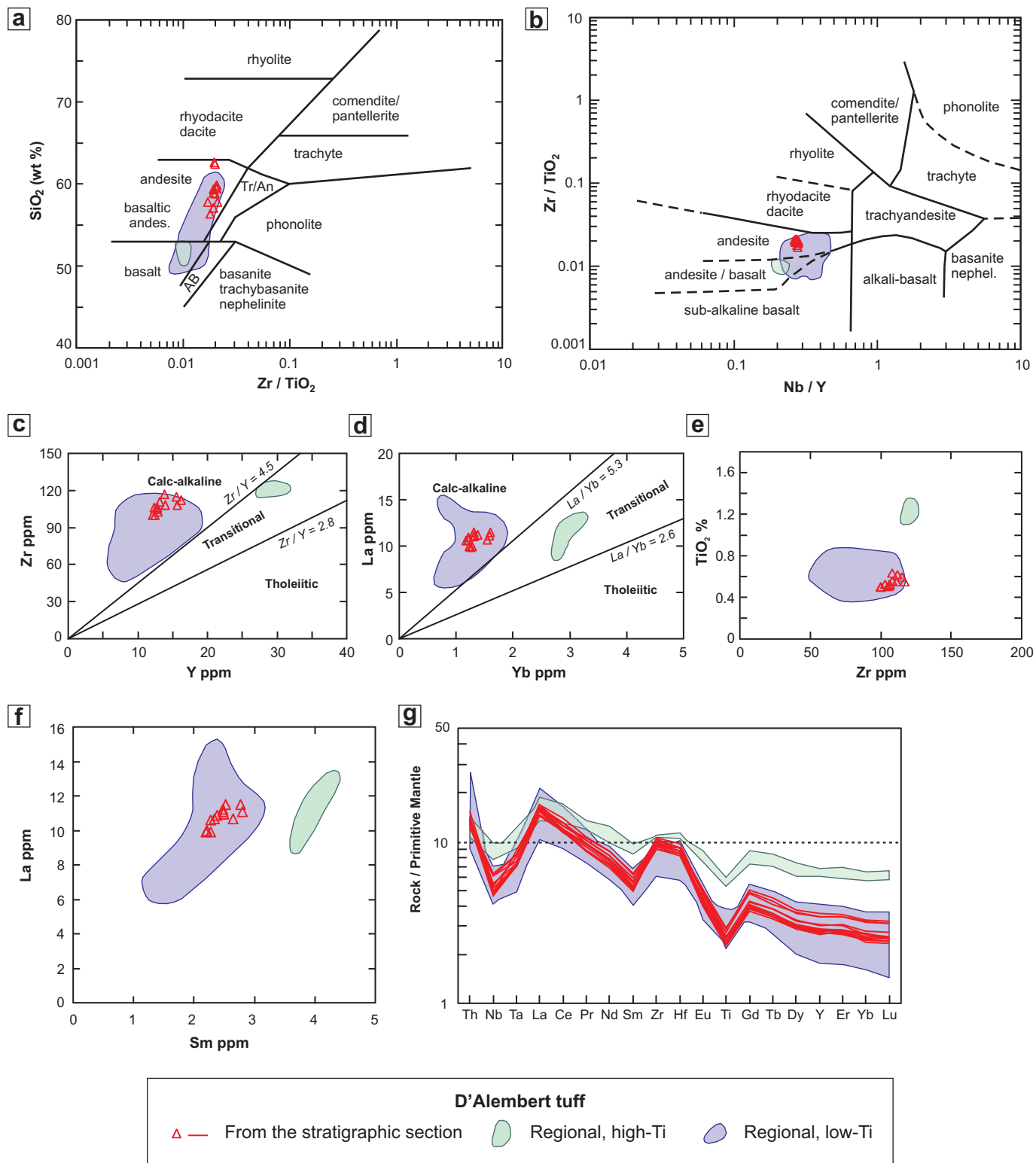


Ross et al, CJES, Fig. 3

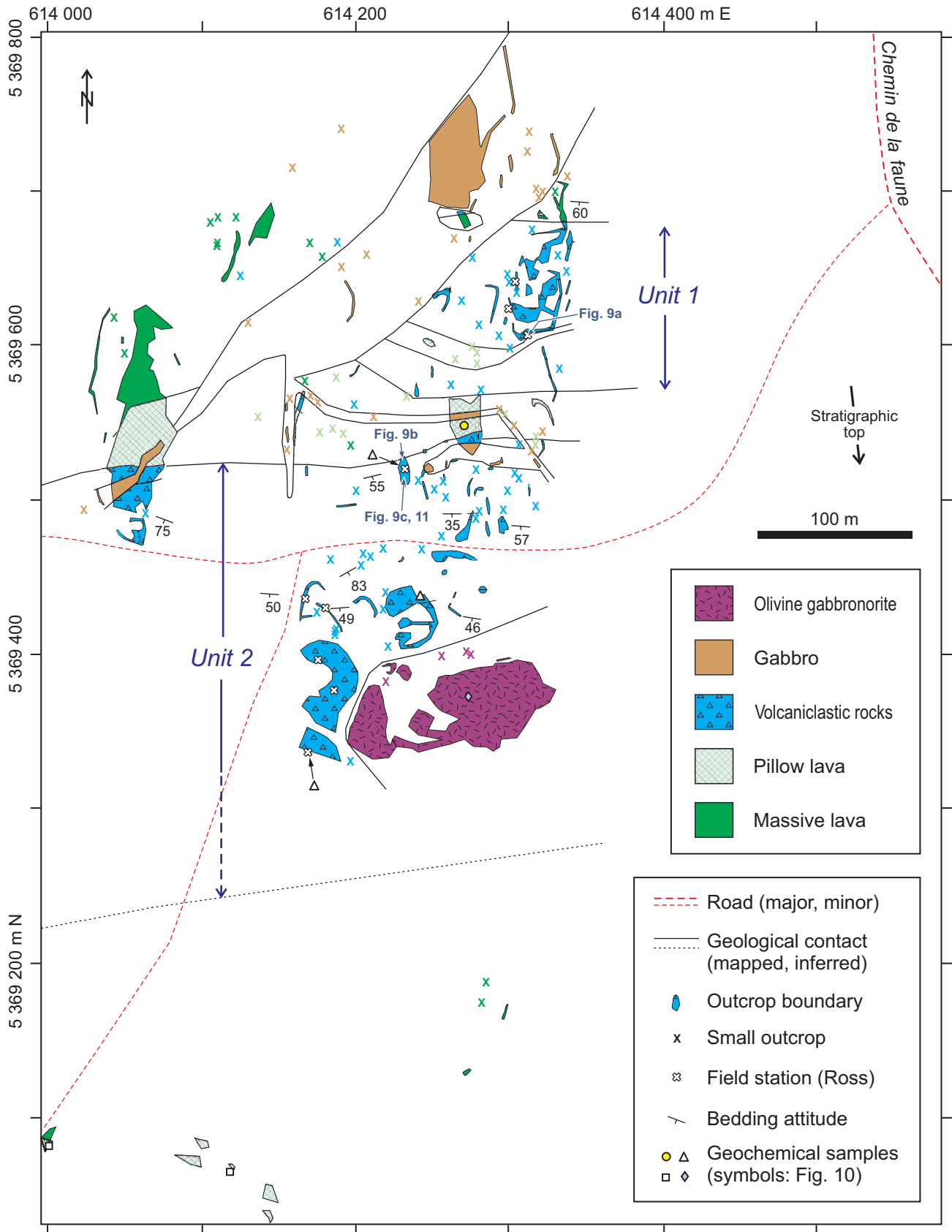






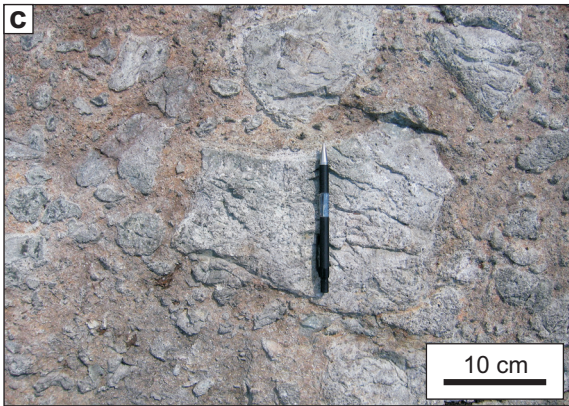
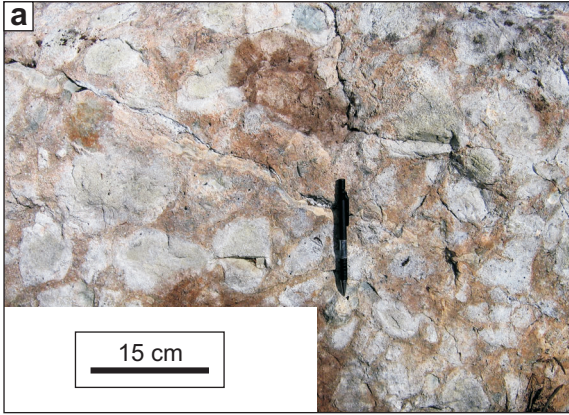


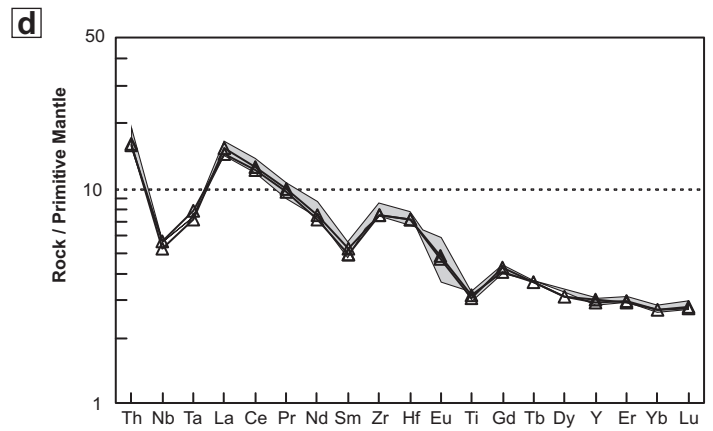
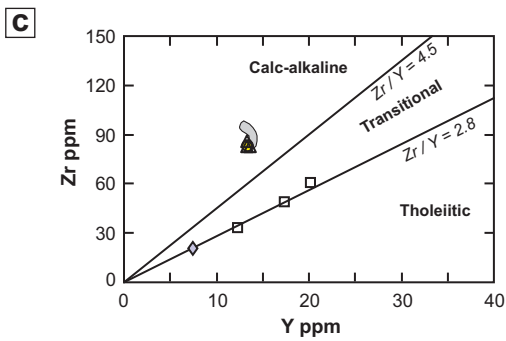
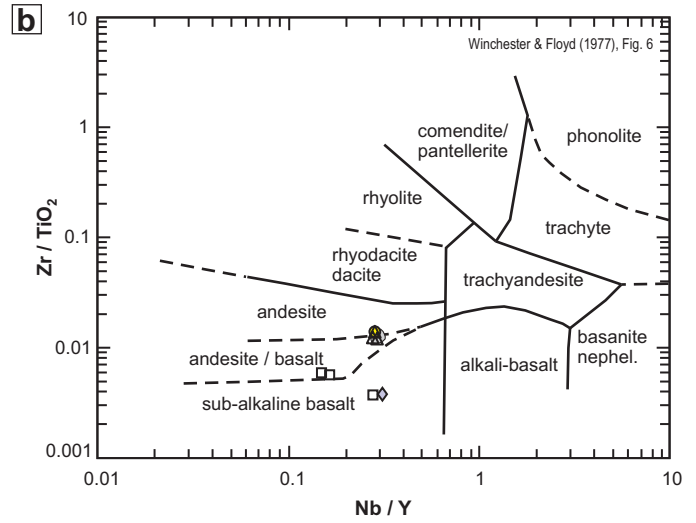
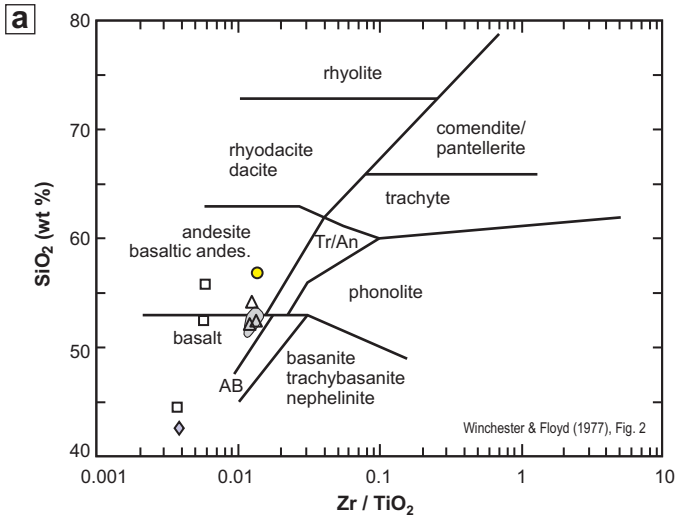




Ross et al. CJES, Fig. 8











**Monsabrais area M3**

- △— Volcaniclastic rock (unit 2)
- Pillow lava between unit 1 and unit 2
- ◐ Field for area M1
- Lavas in southern Fig. 8 and beyond
- ◇ Olivine gabbronorite



**EXPLANATION**

 Covered or poorly exposed (Aug. 07)  
*Intermediate to mafic volcanoclastic rocks*  
 Clasts (drawn to scale)  
 Channel base  
 Tuff or tuffaceous matrix



078 — 55

Fig. 9b

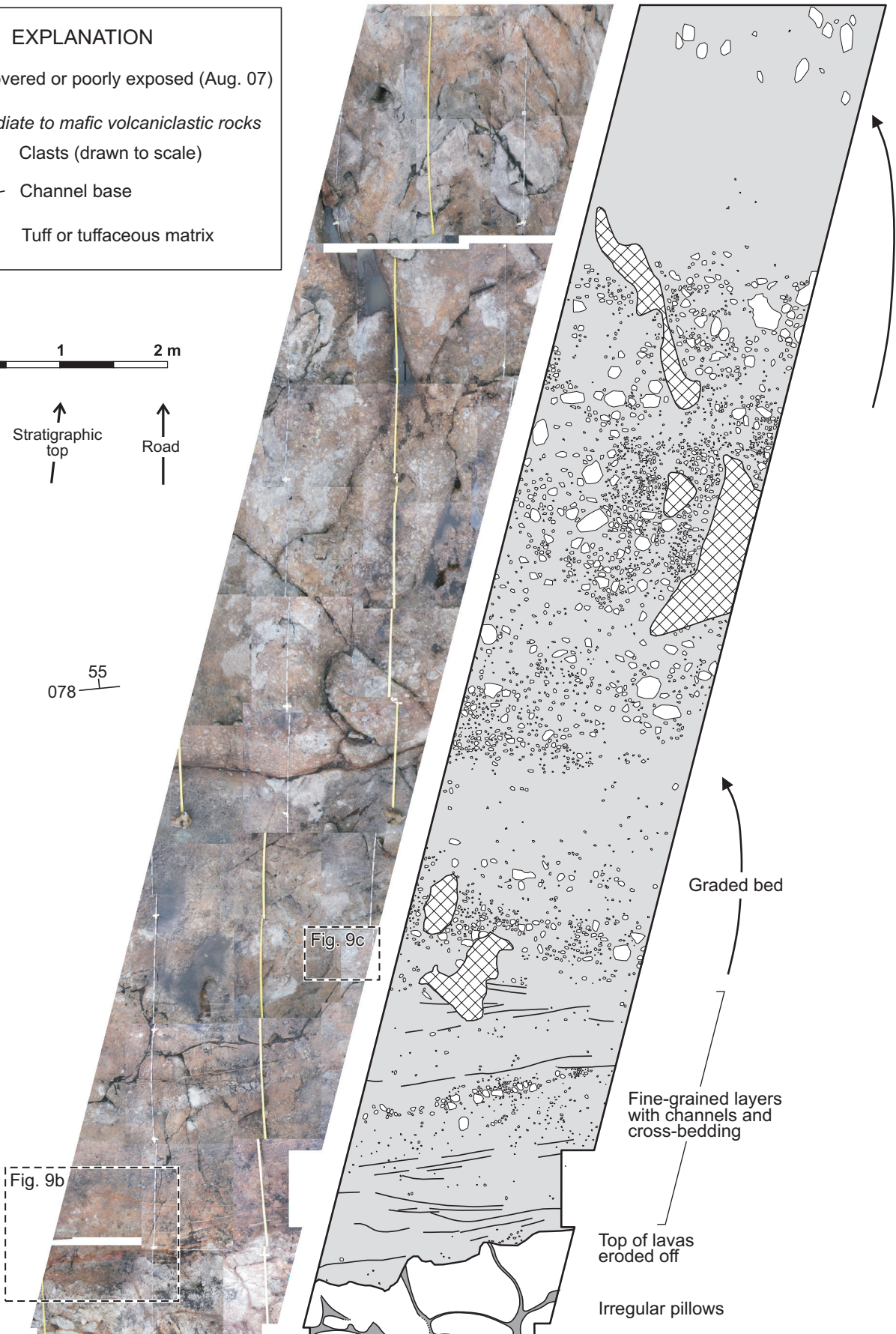
Fig. 9c

Graded bed

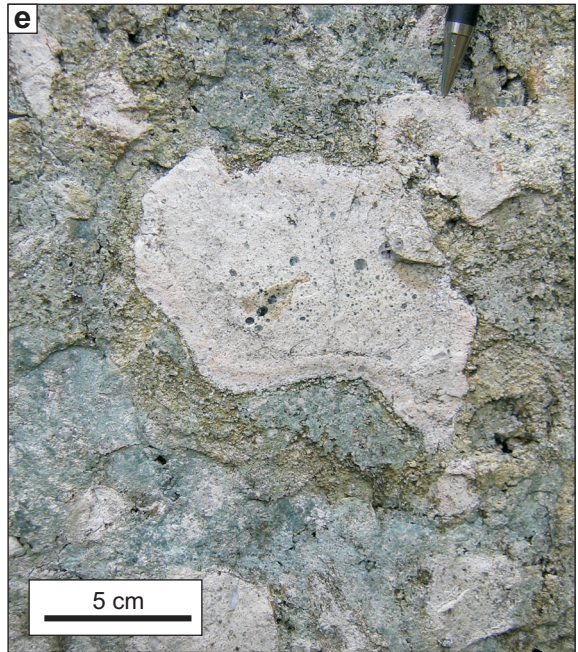
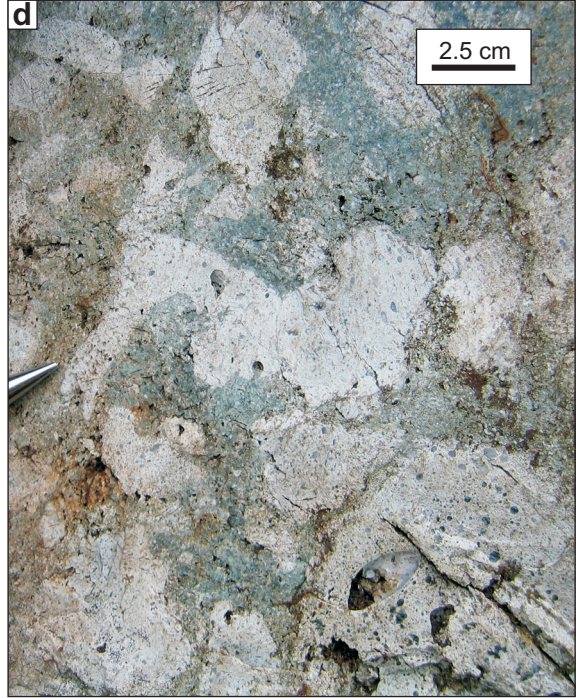
Fine-grained layers with channels and cross-bedding

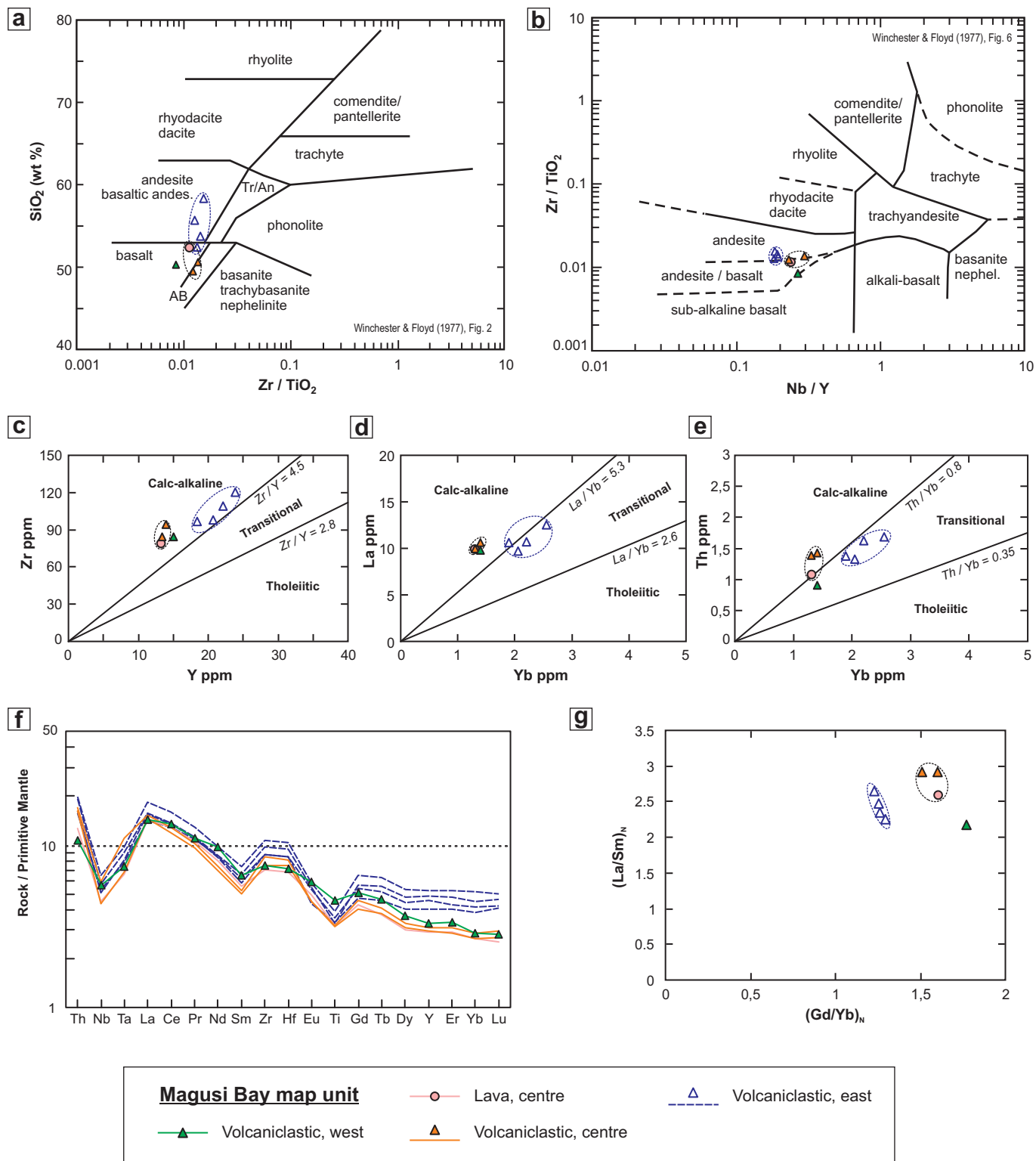
Top of lavas eroded off

Irregular pillows



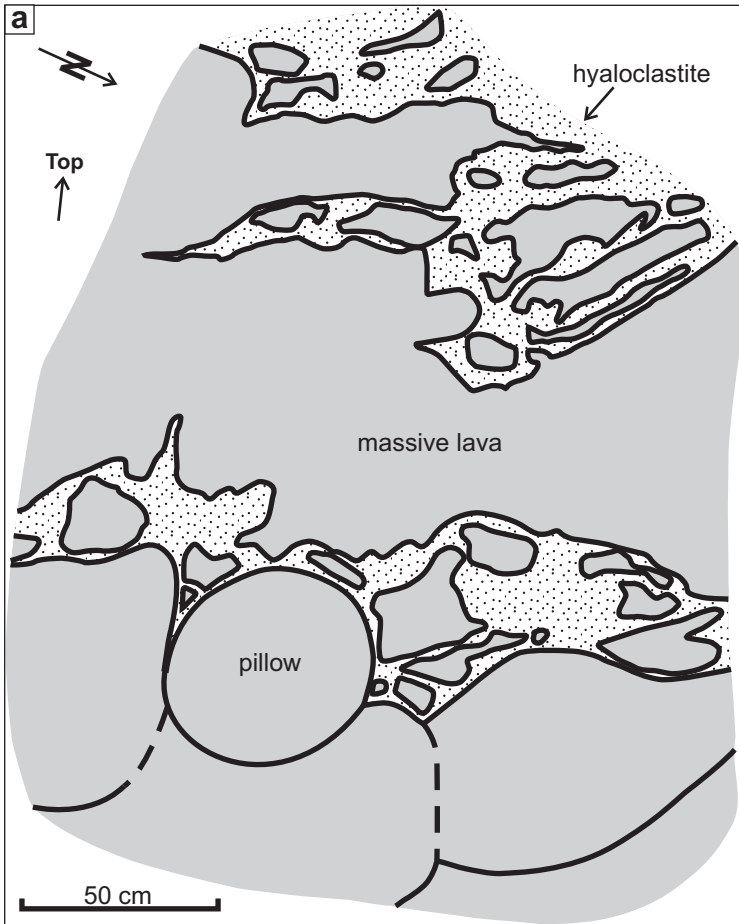


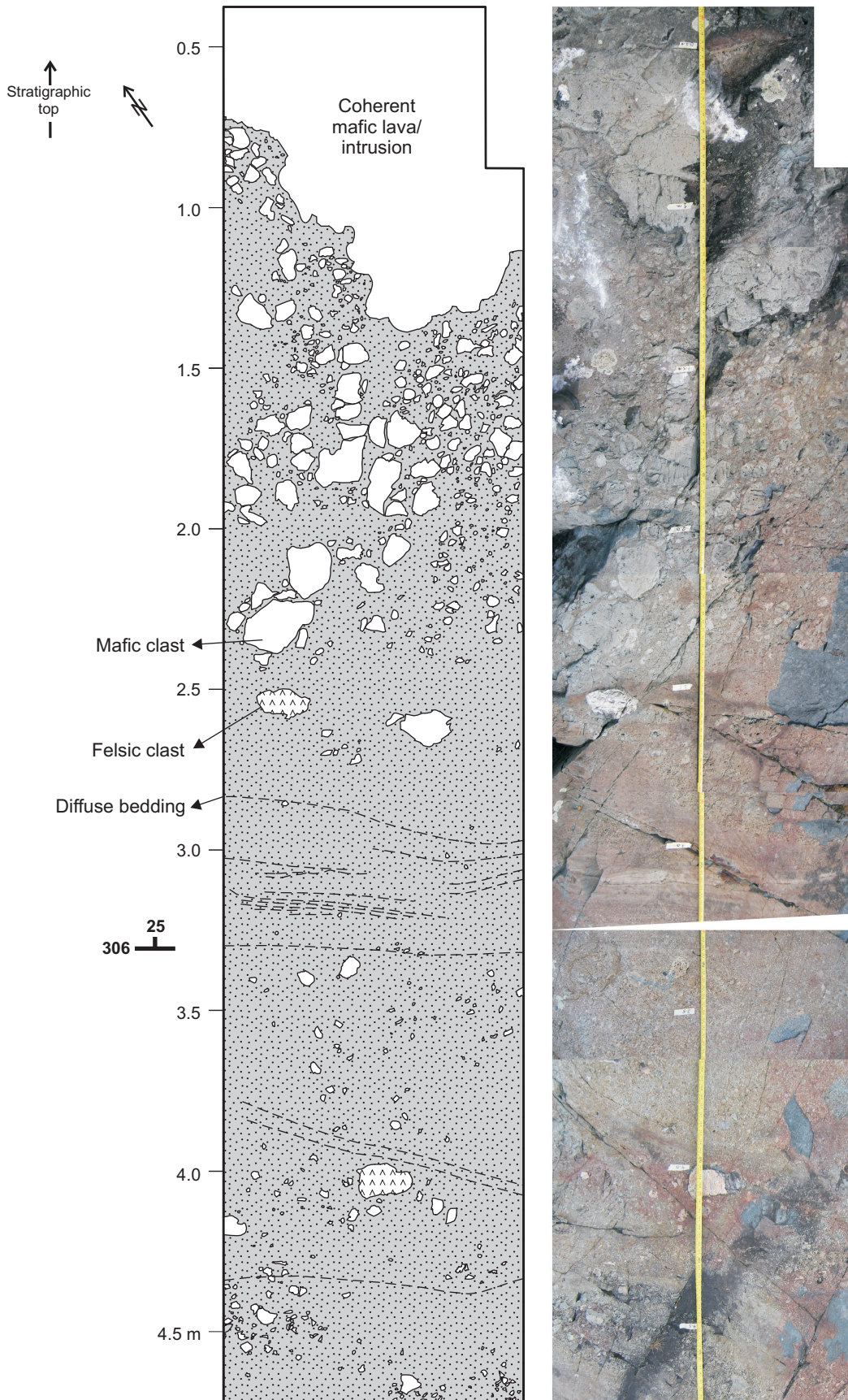




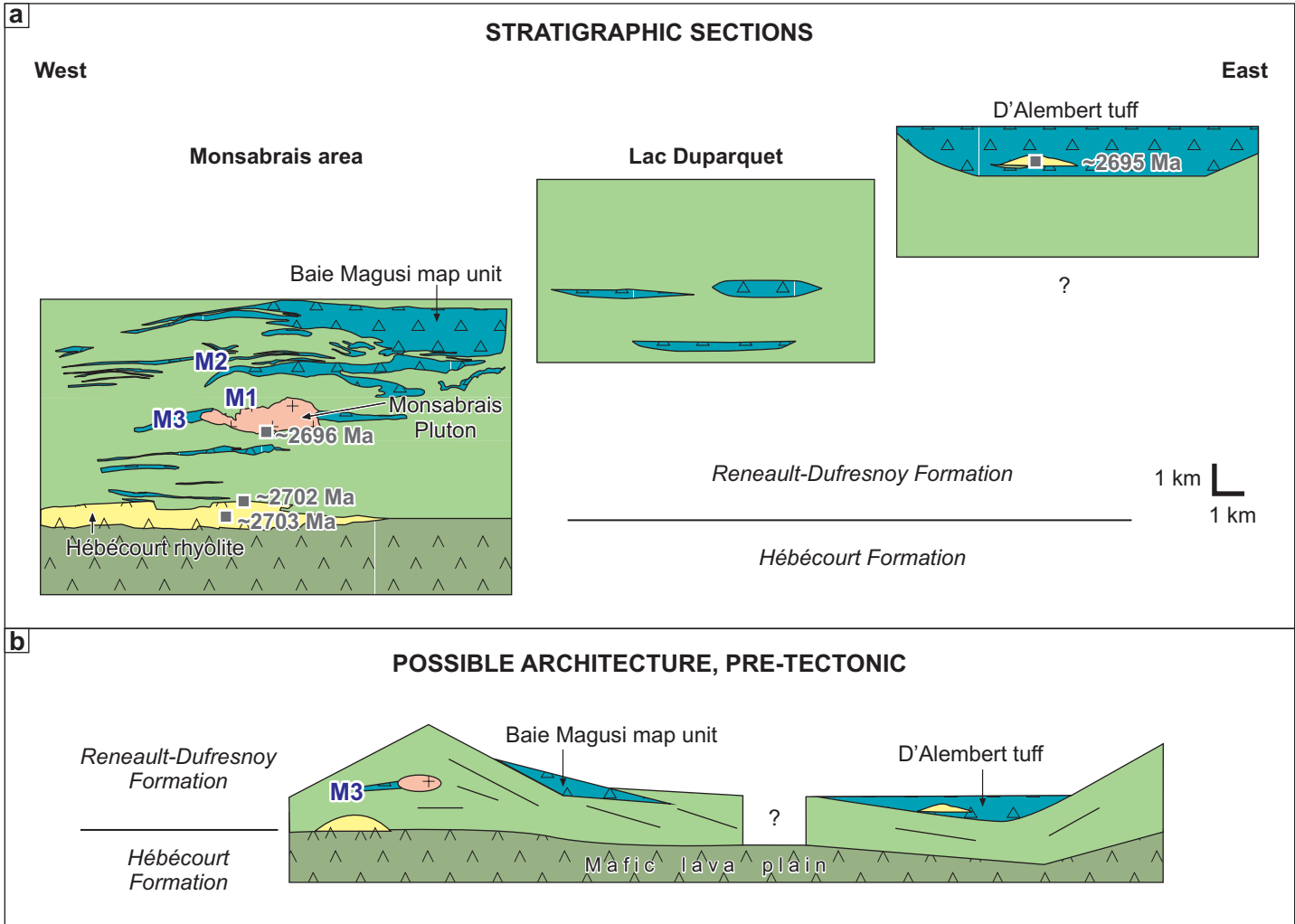
Ross et al. CJES, Fig. 13







Ross et al. CJES, Fig. 15



**APPENDIX: Field stations mentioned in the text and figures**

Station	Easting*	Northing*
06-PSR-017	642 370	5 368 021
06-PSR-172	628 916	5 371 423
06-PSR-174	629 856	5 370 475
06-PSR-189	624 192	5 374 050
07-PSR-067	618 988	5 367 823
07-PSR-070	618 563	5 367 843
07-PSR-133	626 263	5 370 073
07-PSR-138	622 642	5 369 010
07-PSR-169	614 312	5 369 607
07-PSR-170	614 232	5 369 520

\* UTM Nad 83, Zone 17 (measured by GPS)

n/a : not applicable.